Mariele Katherine Faria Motta

The dark universe: observables and degeneracies

O universo escuro: observáveis e degenerecências

Campinas, 2013

Universidade Estadual de Campinas

Instituto de Física Gleb Wataghin

Mariele Katherine Faria Motta

The dark universe: observables and degeneracies

O universo escuro: observáveis e degenerecências

Thesis presented to the Institute of Physics Gleb Wataghin of the University of Campinas in partial fulfillment of the requirements for the degree of Doctor in Science.

Tese apresentada ao Instituto de Física Gleb Wataghin da Universidade Estadual de Campinas como parte dos requisitos exigidos para a obtenção do título de Doutora em Ciências.

Orientador: Prof. Dr. Pedro Cunha de Holanda

Este exemplar corresponde à versão final da tese defendida pela aluna Mariele Katherine Faria Motta orientada pelo Prof. Dr. Pedro Cunha de Holanda.

Campinas, 2013

Ficha Catalográfica
Universidade Estadual de Campinas
Biblioteca do Instituto de Física Gleb Wataghin
Valkíria Succi Vicente – CRB 8/5398

M856d

Motta, Mariele Katherine Faria, 1983-
The dark universe : observables and degeneracies / Mariele Katherine Faria Motta. -- Campinas, SP : [s.n.], 2013.

Orientador: Pedro Cunha de Holanda.
Tese (doutorado) – Universidade Estadual de Campinas, Instituto de Física "Gleb Wataghin".

1.Cosmologia. 2.Universo. 3.Energia escura. 4.Matéria escura (Astronomia). I. Holanda, Pedro Cunha de, 1973- II. Universidade Estadual de Campinas. Instituto de Física "Gleb Wataghin". III. Título.

Informações para Biblioteca Digital

Título em outro idioma: O universo escuro: observáveis e degenerecências
Palavras-chave em inglês:
Cosmology
Universe
Dark energy
Dark matter (Astronomy)
Área de Concentração: Física
Titulação: Doutora em Ciências
Banca Examinadora:
Pedro Cunha de Holanda [Orientador]
Alberto Vasquez Saa
Orlando Luis Goulart Peres
Saulo Carneiro de Souza Silva
Martin Makler
Data da Defesa: 02-08-2013
Programa de Pós-Graduação em: Física

MEMBROS DA COMISSÃO JULGADORA DA TESE DE DOUTORADO DE **MARIELE KATHERINE FARIA MOTTA – RA: 024627** APRESENTADA E APROVADA AO INSTITUTO DE FÍSICA "GLEB WATAGHIN", DA UNIVERSIDADE ESTADUAL DE CAMPINAS, EM 02 / 08 / 2013.

COMISSÃO JULGADORA:

Prof. Dr. Pedro Cunha de Holanda
Orientador da Candidata - DRCC/IFGW/UNICAMP

Prof. Dr. Martin Makler
Centro Brasileiro de Pesquisas Físicas

Prof. Dr. Saulo Carneiro de Souza Silva
IF/UFBA

Prof. Dr. Alberto Vazquez Saa
IMECC/UNICAMP

Prof. Dr. Orlando Luis Goulart Peres
DRCC/IFGW/UNICAMP

Abstract

We would like to explore the consequences of having no prior knowledge about the correct model for dark energy that would allow us to interpret observations. The magnitude of redshift-space distortions and weak gravitational lensing is determined by the metric on which galaxies and light propagate. With precise enough observations it is then possible to use this data to reconstruct the metric on our past lightcone, therefore anisotropic stress and gravitational potentials can be measured in a model-independent way. We explore the dark degeneracy, or the fact that dark matter and dark energy are indistinguishable, for they affect the visible sector only through the gravitational potential they produce. This degeneracy remains unless a dark energy model is provided: the bias between dark matter and galaxies cannot be determined; and only when the Equivalence Principle is valid, one can identify the velocities of dark matter with that of the galaxies. In spite of these limitations, it is possible to construct tests for classes of dark energy models that are based on measurements at different scales and redshifts and do not depend on parametrizations or initial conditions. We demonstrate how one can rule out the most general class of scalar-tensor models without having to assume quasi-staticity. Finally, we discuss how the dark degeneracy manifests itself in a model-dependent analysis.

Resumo

Gostaríamos de explorar as consequências da ausência de conhecimento prévio sobre o modelo correto para energia escura que permita interpretar as observações cosmológicas. A magnitude das distorções no espaço de *redshift* e da lente gravitacional fraca é determinada pela métrica na qual galáxias e luz se propagam. Mostramos que, com observações precisas o suficiente, é possível utilizar estes dados para reconstruir a métrica no nosso cone de luz passado e portanto, o *stress*-anisotrópico e os potenciais gravitacionais podem ser medidos independentemente de modelo. Exploramos a degenerecência escura, ou o fato de que matéria e energia escura são indistinguíveis pois afetam o setor visível apenas através dos potenciais gravitacionais que produzem. Esta degenerecência permanece a menos que se suponha um modelo para energia escura: o *bias* entre galáxias e perturbações de matéria escura não pode ser determinado; e apenas quando o princípio da equivalência é assegurado, pode-se identificar a velocidade da matéria escura com a das galáxias. Mesmo com estas limitações, é possível construir testes para classes de modelos de energia escura que se baseam em medidas em diferentes escalas e *redshifts* e não dependem de parametrizações ou condições iniciais. Demonstramos como se pode descartar a classe mais geral de modelos escalares-tensoriais sem precisar supor a validade do regime quasi-estático. Finalmente, discutimos como a degenerência escura se manifesta em uma análise dependente de modelo.

Contents

Acknowledgments

I would like to thank my collaborators Daniel Boriero, Ignacy Sawicki, Ippocratis Saltas, Luca Amendola, Martin Kunz and Pedro Holanda for their support and many fruitful discussions during my PhD. Other special thanks go to Dorival Netto, Fernando Garcia and Thomas Ruckelshausen for helpful thoughts on this thesis.

Chapter 1

Introduction

1.1 The Dark Sector

According to the Friedmann-Lemaître cosmological model, the Universe is homogeneous, isotropic and has its dynamics determined by the relation between its energy density and the time-scaling of physical coordinates, $a(t)$. A Universe composed by 95% of some invisible dark material and 5% of baryons is in overwhelming good agreement with observations. Moreover, the invisible sector seems to be divided into two very different components, i.e. a pressureless non-baryonic matter, the cold dark matter (CDM), and a misterious dark energy with negative pressure and no time evolution, the cosmological constant Λ. This scenario is known as the ΛCDM model, the concordance model.

Recently analyzed data collected by Planck [1] have shown that our observations are very well fitted by the ΛCDM model. It is important to emphasize that this agreement happens in a model-dependent way. Basically, the testing strategy consists on evolving the six-parameter ΛCDM model in a Boltzmann code, like CAMB [2] or CLASS [3] while fitting the data. But if the dark components are not observable in the first place, which observational evidences have been supporting such model?

Already in the 1920's Slipher and Hubble have found that the observed wavelength of absorption lines of distant galaxies is larger than the wavelength in the rest frame. In the end of the same decade, Hubble have communicated that the stretching of these absorption lines was an indication that the Universe is expanding. He arrived at this conclusion by plotting the velocity v of the receding galaxies versus distance r in what latter was called the Hubble law: $v \simeq H_0 r$ [4]. In the Friedmann Universe, this was and indication that some dark component with negative pressure were acting to drive such expansion. A cosmological constant to be this dark component was not easy to accept, due to its big fine tuning and coincidence problems and still until the 1980's, cosmologists were trying to describe the

Universe's dynamics with matter alone. Without a dark energy component, we would be living in an Einstein-de Sitter Universe, described by the Friedmann equation[1]:

$$\left(\frac{\dot{a}(t)}{a(t)}\right)^2 = H_0^2 \left[\Omega_{m0} a(t)^{-3}\right].$$

By that time, estimates of Ω_m were made, for instance, by inferring the mass that would drive the peculiar motion of galaxies in a certain region of the Universe. This can roughly provide a mean value of mass *per* number of galaxies in this region. By extrapolating this average to the total number of observed galaxies, the approximate value for the total mass in the Universe can be obtained. The observed value of the peculiar velocities was sensibly low, being an indication for one out of two possibilities (when general relativity is assumed): that the mass density is low, so its agglomeration generates a small gravitational effect, or the mass density is high and mass is more homogeneously distributed than galaxies. The second option was soon disregarded, because this would imply that most of the mass would be in the voids between galaxies, leading to formation of irregular galaxies inside the voids, what is not observed. The conclusion, therefore, was that the mass density in the Universe would have to be lower than unity, and consequently, the Einstein-de Sitter model, exclusively composed by matter, was ruled out [5]. Up to today, many other observations have been accumulated as strong indication of dark components, let us briefly review some of them:

Nucleosynthesis

The value of the baryon density today can be measured by comparing the nucleon mass density to the value of the critical density, where the critical density depends on the present value of the Hubble parameter (the local value of the expansion rate). The current limit to this parameter is

$$\Omega_B h^2 = \eta_{10}/273.9 = 0.0229 \pm 0.0012$$

where $\eta_{10} = 6.27 \pm 0.34$ is the baryon to photon ratio and $h = H_0 km.\, s^{-1} Mpc^{-1}$[6]. Clearly, the very small value of Ω_B calls for the presence of non-baryonic constituents.

[1]Let us neglect radiation, since it has such a small contribution at the eras of interest to us: the matter dominated and the dark energy dominated epochs. We will also neglect curvature, since observations indicate that it should be very close to zero.

Rotation curves of galaxies:

The velocities of galaxies flattens out with larger radii, in disagreement with the expected Keplerian fall-off with $V \propto 1/r$ given the observed luminous matter. A possible interpretation for this result is that the baryonic part of the galaxy lives in a halo of dark matter with a density profile that falls of as $1/r^2$ [7, 8].

Clustering of galaxies

As we have mentioned, estimates of the mass that source the gravitational potential driving the motion of galaxies can provide a mean value of mass *per* number of galaxies in this region. This can be extrapolated to the total number of observed galaxies, giving an approximate value for the total matter energy density in the Universe Ω_m, that is found to be around 0.3 [9] . The effect of the deeper potential wells caused by the presence of dark matter on halos can also be probed through X-ray temperature of gas and by weak gravitational lensing of the gravitational potentials [8].

Weak gravitational lensing

The bending of light by a massive object is a prediction of general relativity that gracefully passed the Solar-System tests. The gravitational effect of large-scale structure in our Universe can be tested for by making statistics of the deformation of galaxies' shapes, the so called weak lensing effect. The lensing of galaxies and clusters of galaxies have been a strong indication of non-luminous matter in our Universe. At the end of the 1990's, the analysis of [10] using the frequency of double images of quasars have indicated the presence of dark matter, where the 95% c.l. limits of the total matter energy density were $\Omega_m > 0.38$. More recent analyses often combine different observables, like the galaxy-galaxy lensing + galaxy clustering, carried out by [11] in 2012 with the seventh data release from the Sloan Digital Sky Survey (SDSS) gives $\Omega_m = 0.257^{+0.038}_{-0.034}$ for a ΛCDM fiducial model.

Cosmic Microwave Background

The Cosmic Microwave Background (CMB) is a picture of the Universe when it was only $\sim$ 350.000 years old. Due to the high temperatures at this epoch, photons, baryons and electrons were tightly coupled through Coulomb and Compton interactions. As expansion causes the Universe to cool down to approximately $1\,eV$, the photons are released to freely move through space. The Cosmic Microwave Background is important to confirm the averaged homogeneity of the Universe, because it is described by a black body spectrum to 1 part in 10^5. Nonetheless,

the most important features of the CMB are its anisotropies, they reveal characteristics of the perturbed Universe and connect many physical parameters through one single observable [4].

In fact, the most striking agreement of the ΛCDM model with observations comes from the Planck mission, launched in 2009, from which maps and data analyses were released in early 2013. The Planck mission has measured with high precision the Cosmic Microwave Background temperature and its anisotropies and combined this with the lensing-potential power spectra. By fitting observations with the six-parameter ΛCDM model, the data analysis favors a scenario where the energy densities of baryons and cold dark matter are estimated (at 68% confidence level) to be$\Omega_c h^2 = 0.1199 \pm 0.0027$ and $\Omega_b h^2 = 0.022050 \pm 0.0028$ ($H_0 = 100h\, km\, s^{-1} Mpc^{-1}$), respectively, and a seemingly low value (in comparison to other probes) of the Hubble constant, $H_0 = 67.3 \pm 1.2$, with a total matter density parameter, $\Omega_m = 0.315 \pm 0.017$ [1].

Structure Formation

Gravitational instability has created density perturbations that have collapsed forming the galaxies and clusters that we see today. In order to have the observed structures, perturbations must have gone non-linear before the present epoch. The electromagnetic pressure of baryons delays the structure formation, therefore the observational scenario favors a Universe dominated by a pressureless dark matter. This is evident through, e.g. the matter the power spectrum (whose normalization depends on the measured value of H_0), i.e. the turnover of the power spectrum depends on the total matter energy density, therefore also on the energy density of dark energy. The matter power spectrum also presents wiggles around $k \simeq 0.1\, h\, Mpc^{-1}$, from the baryon acoustic oscillations, that depend on the fraction Ω_b/Ω_m [12].

Supernovae

A Supernova type Ia (SNIa) explodes when a white dwarf in a binary system exceeds the Chandrasekhar limit, giving rise to a very luminous event. The absolute magnitude of the luminosity can be correlated with the width of the light curve. Thus, by observing the apparent magnitude and the light curve simultaneously, one can infer the absolute magnitude, that is, in plinciple, a known value at the peak of brightness. Assuming that this is so for every SNIa, making them standard candles, one can further infer the luminosity distance through the relation between the apparent and the absolute magnitudes. With this assumption, type Ia Supernovae have provided evidence that the Universe is expanding with an acceleration,

making the case for a dark energy component [4, 13].

Let us call the attention for the fact that all measurements of Ω_m have to be normalized. This can be easily seen in the Friedmann equation, where we can define the critical density as $\rho_{cr} \equiv H_0^{-2}$, being therefore determined by local measurements of the expansion. We also want to remark that, in spite of SNIa constituting evidence for the acceleration, there is still space for something different than a cosmological constant, because one can always reproduce the expansion history by exploring the degeneracy between the dark energy equation of state and the matter energy density, as will be argued in part II.

1.2 Current picture of the dark side

Dark Issues

As it is well known, one of the ingredients of the standard model, the cosmological constant, suffers from two problems, the fine tuning and the coincidence problem. A natural candidate for a cosmological constant is the vacuum energy of particles and, in fact, there is no way to distinguish both components. In order to explain the accelerated expansion, the vacuum energy density should be of order $E_{vac}^{(obs)} \simeq (10^{-3}eV)^4$. On the theoretical side, the value for this energy density comes from the contribution from the zero-point quantum-mechanical vacuum fluctuations of each particle in the standard model, being of the order of $E_{vac}^{(theo)} \simeq (10^{27}eV)^{42}$, 120 orders of magnitude larger than the observed value. It is interesting to remark that energy density has units of $[energy]^4$, by expressing this value in terms of a mass scale $\rho_{vac} = M_{vac}^4$, the discrepancy is of 30 order of magnitude in energy scale. It is possible to attenuate the fine tuning problem in supersymmetric (SUSY) scenarios where supersymmetry is spontaneously broken at a low scale, and the vacuum energy is then set by the scale at which SUSY is broken. If supersymmetry is preserved until the weak scale, then $M_{vac} \approx M_{SUSY} \approx 10^3 GeV = 10^{12}eV$, only 15 orders of magnitude above the observed, but a large discrepancy remains [13, 14]. The second problem with the cosmological constant is that its energy density and that of matter are of the same order of magnitude today, although they scale differently in time. From the anthropic point of view, one could argue that such coincidence is not a problem, i.e. that the energy density of dark energy is the highest value that still allows for structure formation, therefore life itself [4].

Let us not forget that dark matter also presents a coincidence problem, i.e. the energy density of dark matter and baryons are too, of the same order of magnitude, although, in

[2]With a cutoff at the Planck scale, introduced because the contribution from the high frequency modes is divergent.

principle, they are produced in very different fashions. Baryons are produced by an out of equilibrium, non-thermal process and dark matter candidates are, in general, supposed to be thermally produced, i.e. the right abundance of dark matter can be obtained via thermal production in weak interactions. Other difficulties to conciliate the cold dark matter scenario with observations are the missing satellites and the cuspy core problems [8]. As we will discuss in more details in chapter 8, this has motivated the appearance of warmer dark matter candidates in the picture.

Direct detection

The dark components make up most of the energy density of the Universe, and yet they have been inferred only by their gravitational interaction on very large scales: the Hubble horizon (both dark matter and dark energy) and the galaxy size (dark matter only). Any prospect of direct detection of the dark components would remove them from the darkness.

If dark matter is directly detected, it could be brought to the same status as baryons, where the abundance and, therefore the energy density,s could be predicted. At the moment, the most promising dark matter candidate is a Weakly Interacting Massive Particle, or wimp. Extensions of the particles standard model, like supersymmetric theories, are able to predict plausible candidates for wimps. The combined constraints from the underground laboratories CDMS (Cryogenic dark matter Search) and EDELWEISS for a wimp with mass of $90GeV$ exclude a cross section of $3.3 \times 10^{-44} cm^2$ at 90% C.L. For larger masses, above $700GeV$, there is some improvement in the limits by a factor of 1.6 [15]. Non-wimp dark matter candidates are, e.g. gravitinos, axions, superwimpS and sterile neutrino, for more on this, we point to [16] and the review [17].

The landscape of dark energy detection through non-gravitational interactions is still not very large. If not protected by some symmetry, a dark energy particle should be coupled to all other forms of matter by quantum corrections [18], potentially leading to violations of the Equivalence Principle, fifth forces and variations of coupling constants, like the fine structure constant α. Such fifth-forces and time variation of α could be used to detect a dynamical dark energy field [14, 19]. In the CMB, for example, a different value of α can shift the position of the first acoustic peak, that is inversely proportional to the sound horizon at last scattering. If α increases, so increases the value of the redshift of last scattering, generating a bigger early Integrated Sachs-Wolfe effect. As a consequence, the first acoustic peak will also present a higher amplitude [4]. In the Planck analysis, the limits on the time-variation of α from the redshift of $z \sim 10^3$ to today, is constrained to be less the 0.4% [1], and spatial variations of α seem to be excluded [20].

Additionally, if dark energy is a dynamical scalar field, its mass is constrained to be of

order of the Hubble scale $m_\phi \sim H_0 \sim 10^{-33} eV$ [3]. With such small mass, this scalar field would mediate a long range force with standard model particles. However, local gravity experiments designed to test the Equivalence Principle constrain this fifth-force to be small [21]. Notwithstanding, a recent dark energy candidate, the Chameleon scalar field [22], has the property that its mass can change according to the medium. In particular, it presents a larger mass in larger density environments. This type of scalar field is therefore able to evade local fifth-force constrains. Results from the GammeV Chameleon Afterglow Search constrain the (dimensionless) coupling of Chameleons to photons to be smaller than 5 orders of magnitude. The coupling to matter is also excluded between 4 to 12 orders of magnitude [23].

1.3 Observational prospects and Motivations

After decades of observations and data analysis, the continuous confirmation of the ΛCDM model, in particular for favoring the existence of exotic components, is overwhelming, if not disturbing. Independently of the underlying reality that observations are able or not to reveal, such unexpected picture is an indication that our research is mostly guided by data, not prejudice. This emphasizes the importance of how do we interpret observations; the importance of having good quality data, with range and precision; and, finally, the importance of developing strategies to constrain theories from observations.

The cosmological constant problem is probably the main issue that has driven researchers to look for other models to describe the dynamics of the Universe. Alternative proposals for dark energy or modifications of gravity, however, are more than just attempts to fix specific disagreements, for they potentially explore a larger theoretical space, therefore demanding a richer data space in order to distinguish between theories. When something other than a simple cosmological constant is considered, new features are potentially introduced. Such novel aspects might be not properly accounted by a standard analysis.

At the moment, satellite surveys and telescopes, like the Sloan Digital Sky Survey (SDSS) [24], dark energy Survey (DES) [25], Panoramic Survey Telescope & Rapid Response System (Pan-Starrs) [26] are collecting data on our Universe to be released within a few years. They

[3] This is a consequence of the equation of motion for the scalar field of mass m in an expanding Universe.

$$\ddot{\phi} + 3H\dot{\phi} + m^2\phi + ... = 0$$

If the field's mass is much smaller than the Hubble parameter, the friction term dominates the dynamics and would not produce a significant change in the fine structure constant. On the other hand, for a mass much larger than H, the field would start to oscillate early in the history of the Universe, slowly rolling to the potential minimum.

present an improvement on sensitivity, sky-coverage, cosmological scale, redshift and precision. Within less than a decade, the European Space Agency (ESA) will launch the Euclid satellite [27], which is the successor of WMAP (NASA) and Planck Survey (ESA/NASA) satellites in the sense that it is being built to address the dark sector of the Universe. Euclid will measure the shapes of over a billion of galaxies and accurate spectra of tens of millions of galaxies out to redshift $z = 2$ and it has been designed to have precision to break degeneracies and distinguish between important dark energy models [28].

With such promising prospects, we have the opportunity to improve the scientific return of such missions. In this work we explore an alternative approach to test for models: First, we identify which quantities are observable without assuming a dark energy model. Afterwords, we apply null-tests to data by using measurements of the identified observables scale by scale, redshift by redshift, not requiring parametrizations or initial conditions. This differs from the common approach, that is basically to evolve parametrized quantities in a Boltzmann code while fitting the data. We also discuss the dark degeneracy problem, or the fact that, so far, as both dark matter and dark energy have been detected only through their gravitational effect, one can only constrain the combined dark fluid, not each component separately.

This thesis expands and details some of the results and arguments presented in references [29, 30, 31] and it is organized as follows:

In chapter 2, we illustrate the change introduced by dark energy by presenting the Einstein equations of a general dark energy fluid characterized by its energy density, pressure, heat flow and anisotropic stress. In chapter 3, we present a minimal set of assumptions that are required to interpret cosmological observations and; in chapter 4, based on these assumptions, we determine which observable quantities can be extracted from observations at background (section 4.1) and linear perturbation level (section 4.2). Untill this point, no novel result has been presented, but we would like to emphasizer the different persective that we take, by identifying potentially observable quantities without attempting to connect observations with the dark matter perturbations, which are unknown. So in section 4.4, we recover the standard approach to observations and the observables we have identified with dark matter perturbations. Our original contribution starts in chapter 5, where we develop consistency relations between observable quantities. We show how the consistency relations can be used as null-tests of different models in chapter 6. Particularly, we demonstrate how anisotropic stress offers an extra handle to fully constrain all scalar-tensor models which exhibit such feature. We also argue that if anisotropic stress is not observed, a consistency check can be used as a model-dependent null-test of a specific theory, as we work out for k-*essence* (section 6.1). In chapter II we make and interlude and discuss the dark degeneracy, expressed as the unobservability of the dark matter properties and as a degeneracy between parameters in a

model-dependent analysis. In chapter 7, we present our conversion model of cold dark matter into dark radiation that exhibits this parameter degeneracy. Finally, in chapter 8 we discuss our results.

Notation and symbols

We use overdots and primes respectively as derivatives with respect to time and the logarithm of the scale parameter ($N \equiv ln\, a$); and units such that $c = 8\pi G = 1$. For the sake of simplicity, we will work in Fourier space. In part I, we will consider the wavenumber k to be the physical wavenumber $k \equiv k_{phys}/aH$, expressed in units of the cosmological horizon, therefore it is a time-dependent quantity, whereas in part II, k is just the "normal" wavenumber.

Part I

Dark energy

Chapter 2

Dark energy Perturbations

Dark energy refers generally to what causes the Universe's expansion to accelerate, not restricted to be a cosmological constant. As one considers a general dark energy in the cosmic scenario, many assumptions behind the concordance model can be relaxed. In the ΛCDM model, the only component capable of clustering is dark matter[1], and dark energy is a smooth, static quantity. In a general scenario, the background evolution can differ, (as we will discuss in part II), however one can always reproduce the expansion history by tuning the equation of state. Actually, many dark energy models are built to agree on the background level. Therefore, the most important change happens on the perturbative level, because dark energy can potentially cluster, changing completely the analysis of the perturbed theory. Besides, since the background is not enough to distinguish between models, we need to evaluate their signature on structure formation.

In order to illustrate that, we will review the perturbed equations of motion in a Universe filled with dark matter only and then present the same equations for a general fluid. Throughout this thesis, we will consider a Universe that is, in average, homogeneous and isotropic and has small (linear) perturbations, described by the Friedmann-Lemaître-Robertson-Walker metric (FLRW, from now on):

$$\mathrm{d}s^2 = -(1+2\Psi)\mathrm{d}t^2 + a^2(t)(1+2\Phi)\mathrm{d}\boldsymbol{x}^2\,. \tag{2.0.1}$$

We chose to work in the gauge-invariant newtonian gauge. The scalar metric potentials Φ and Ψ are therefore, potentially observables. The choice of gauge implies we are treating only scalar perturbations. Since only the scalar modes couple to matter and we are interested in extracting the observables from structure formation, the gauge choice is justified.

[1]Here we don't distinguish between dark matter and baryons. Galaxies for us are shiny objects that trace perturbations, whose shapes and number density can be used to test for relativistic effects.

2.1 Dark matter perturbations

As it is well known, dark matter can be described by a pressureless perfect fluid, with Energy-Momentum Tensor (EMT) given by:

$$T^{(m)}_{\mu\nu} = \rho\, u_\mu u_\nu, \tag{2.1.1}$$

where ρ is the matter energy density. The perturbed form of the EMT is then given by

$$\delta T^{(m)}_{\mu\nu} = \rho\,(u_\mu \delta u_\nu + \delta u_\mu u_\nu) + \delta\rho\, u_\mu u_\nu. \tag{2.1.2}$$

From now on, δ stands for the perturbation of the quantities in question, and the four-velocity is defined, up to first order, as

$$u^\mu \equiv \left[\frac{1}{a}(1-\Psi), \frac{v^i}{a}\right], \tag{2.1.3}$$

$$u_\mu = g_{\mu\nu}u^\nu = \left[-a(1+\Psi), a v^i\right]. \tag{2.1.4}$$

The perturbed Einstein equations in a scenario where only dark matter has perturbations are given by:

- Poisson Equation (Hamiltonian constraint):

  δG_{00}=δT_{00}

$$2\frac{k^2\Phi}{a^2} + 6H\dot{\Phi} - 6H^2\Psi = \delta\rho_m\,, \tag{2.1.5}$$

- Momentum Constraint:

  $\delta G_{0i} = \delta T_{0i}$

$$2\frac{k^2}{a^2}\left(\dot{\Phi} - H\Psi\right) = -\rho_m\theta, \tag{2.1.6}$$

where we used the definition of the divergence of the velocity

$$\theta \equiv ik_i\delta u^i = \nabla_i v^i. \tag{2.1.7}$$

- Anisotropy Constraint (Traceless part of Einstein equations):

  $\delta G^i_j - {}^1\!/_3\delta^i_j\delta G^k_k = \delta T^i_j - {}^1\!/_3\delta^i_j\delta T^k_k$

$$\Phi + \Psi = 0\,. \tag{2.1.8}$$

The Covariant conservation of the EMT leads to

- Energy conservation:

  $\nabla^\mu G_{\mu 0} = \nabla^\mu T_{\mu 0}$

$$\dot{\delta\rho} + 3H\delta\rho + \rho\left(\theta + 3\dot{\Phi}\right) = 0\,, \tag{2.1.9}$$

and

- Momentum conservation:

  $\nabla^\mu G_{\mu i} = \nabla^\mu T_{\mu i}$

$$\dot{\theta} + 2H\theta - \frac{k^2}{a^2}\Psi = 0. \tag{2.1.10}$$

In order to find the evolution for dark matter perturbations $\delta_m = \frac{\delta\rho}{\rho}$, one can simply divide equation Eq(2.1.9) by ρ, solve it for Θ and substitute in Eq(2.1.10), resulting

$$\ddot{\delta_m} + 2H\dot{\delta_m} = -\frac{k^2}{a^2}\Psi + 3\left(\ddot{\Phi} + 2H\dot{\Phi}\right)\,. \tag{2.1.11}$$

As we will see, to find the evolution equation for dark energy perturbations turns out to not be so simple.

2.2 Dark energy perturbations

We now present the linearly perturbed Einstein equations for a general single fluid minimally coupled to gravity in addition to the dark matter fluid. By considering minimal coupling, we assure covariant conservation of the fluid's energy momentum tensor. The energy momentum tensor of the fluid is described by its energy density $\mathcal{E}$, pressure $\mathcal{P}$, energy flow q and anisotropic stress [2]π:

$$T^{(x)}_{\mu\nu} = (\mathcal{E} + \mathcal{P})u_\mu u_\nu + g_{\mu\nu}\mathcal{P} + q_\mu u_\nu + q_\nu u_\mu + \tau_{\mu\nu}\,, \tag{2.2.1}$$

The Einstein equations for this fluid are:

- Poisson Equation (Hamiltonian Constraint):

  δG_{00}=δT_{00}

$$2\frac{k^2\Phi}{a^2} + 6H\dot{\Phi} - 6H^2\Psi = \delta\mathcal{E} + \delta\rho_m\,, \tag{2.2.2}$$

- Momentum Constrain:

  $\delta G_{0i} = \delta T_{0i}$

[2]We follow the notation used in [32]

$$2\frac{k^2}{a^2}\left(\dot{\Phi} - H\Psi\right) = -(\rho_m + \mathcal{E} + \mathcal{P})\theta + \frac{k^2\delta q}{a^2} - \dot{q}\theta, \tag{2.2.3}$$

- Anisotropy Constrain (Traceless part of Einstein equations):

  $\delta G^i_j - {}^1\!/_3\delta^i_j\delta G^k_k = \delta T^i_j - {}^1\!/_3\delta^i_j\delta T^k_k$

$$\Phi + \Psi = \delta\pi\,. \tag{2.2.4}$$

The Covariant conservation of the EMT leads to

- Energy conservation:

  $\nabla^\mu G_{\mu 0} = \nabla^\mu T_{\mu 0}$

$$\dot{\delta\mathcal{E}} + 3H\left(\delta\mathcal{E} + \delta\mathcal{P}\right) + \left(\mathcal{E} + \mathcal{P}\right)\left(\theta + 3\dot{\Phi}\right) - \frac{k^2\delta q}{a^2} + \dot{q}\theta = 0\,, \tag{2.2.5}$$

and

- Momentum conservation:

  $\nabla^\mu G_{\mu i} = \nabla^\mu T_{\mu i}$

$$\left(\mathcal{E} + \mathcal{P}\right)\left(\dot{\theta} + 2H\theta - \frac{k^2}{a^2}\Psi\right) - \frac{k^2}{a^2}\delta\mathcal{P} + \Theta\dot{\mathcal{P}} - \tag{2.2.6}$$

$$3H\left(\frac{k^2}{a^2}\delta q - \dot{q}\theta\right) - \frac{1}{a^2}\left(k^2\delta q - a^2\dot{q}\theta\right)^{\cdot} - \frac{2}{3}\frac{k^4}{a^4}\delta\pi = 0. \tag{2.2.7}$$

In order to evaluate the impact of dark energy perturbations on strucure formation, we should obtain the evolution equation for dark energy perturbations $\delta_x = \frac{\delta\mathcal{E}}{\mathcal{E}}$. Notice however, that this is not straightforward as in the dark matter case, because we have, besides $\delta\mathcal{E}$ and Θ, pressure perturbations $\delta\mathcal{P}$, heat flux, q and anisotropic stress $\delta\pi$, that are not known *a priori*.

In order to obtain the evolution of dark energy perturbations, we should furnish closure relations between $\delta\mathcal{E}$, $\delta\mathcal{P}$ and $\delta\pi$. For an adiabatic perfect fluid, where q and π vanish, the closure relation is given by the sound speed:

$$\delta\mathcal{P} \equiv c_s^2\delta\mathcal{E}. \tag{2.2.8}$$

From observations, we can not say which kind of fluid describes dark energy, so we can not furnish such closure relations. What one could try is to develop a parametrization that implies a closure relation and test for values of these parameters [3].

[3] This is what is done for ΛCDM, where all the parameters for the DE perturbations are set to zero.

What we would like to point out here, by using the more intuitive fluid formalism, is just the complexity that it is introduced by dark energy, and how it changes completely our point of view on perturbations. We summarize the equations of motion in table 2.1.

It is interesting to notice that, in the literature of many dark energy models, the dynamics of these perturbations are often neglected. As acknowledged by Kunz and Sapone in [33], the main effect of dark energy can be the change of the background, expressed through the evolution of $H(z)$, however, the gravitational potential Ψ will also present a different evolution once dark energy perturbations are included. Normally, dark energy perturbations are assumed to be unimportant, and this can be a good assumption for a scalar field dark energy, because the high sound speed in this case prevents clustering on basically all scales. Nonetheless, if the sound speed is small, what is not excluded by observations (even negative values), the growth of dark energy perturbations can be significant.

The equations that govern the growth of both dark components are two coupled differential equations. The evolution equation for each component is connected through the gravitational potential. Therefore, in order to fully characterize the growth of dark matter perturbations, one should actually take the evolution of DE perturbations into account. What is usually done is to completely neglect the effect of dark energy perturbations in the potentials that source the growth of dark matter perturbations.

Table 2.1: Comparing the linear perturbation equations for dark matter and dark matter + dark energy fluid.

Einstein Equation	**Poisson**
CDM	$2\frac{k^2\Phi}{a^2} + 6H\dot{\Phi} - 6H^2\Psi = \delta\rho_m$
+ dark energy	$2\frac{k^2\Phi}{a^2} + 6H\dot{\Phi} - 6H^2\Psi = \delta\mathcal{E} + \delta\rho_m$
	Hamiltonian
CDM	$2\frac{k^2}{a^2}\left(\dot{\Phi} - H\Psi\right) = -\rho_m\theta$
+ dark energy	$2\frac{k^2}{a^2}\left(\dot{\Phi} - H\Psi\right) = -(\rho_m + \mathcal{E} + \mathcal{P})\theta + \frac{k^2\delta q}{a^2} - \dot{q}\theta$
	Anisotropy
CDM	$\Phi + \Psi = 0$
+ dark energy	$\Phi + \Psi = \delta\pi$
	Energy Conservation
CDM	$\dot{\delta\rho} + 3H\delta\rho + \rho\left(\theta + 3\dot{\Phi}\right) = 0$
+ dark energy	$\dot{\delta\mathcal{E}} + 3H\left(\delta\mathcal{E} + \delta\mathcal{P}\right) + \left(\mathcal{E} + \mathcal{P}\right)\left(\theta + 3\dot{\Phi}\right) - \frac{k^2\delta q}{a^2} + \dot{q}\theta = 0$
	Momentum Conservation
CDM	$\dot{\theta} + 2H\theta - \frac{k^2}{a^2}\Psi = 0$
+dark energy	$\left(\mathcal{E} + \mathcal{P}\right)\left(\dot{\theta} + 2H\theta - \frac{k^2}{a^2}\Psi\right) - \frac{k^2}{a^2}\delta\mathcal{P} + \Theta\dot{\mathcal{P}} -$ $3H\left(\frac{k^2}{a^2}\delta q - \dot{q}\theta\right) - \frac{1}{a^2}\left(k^2\delta q - a^2\dot{q}\theta\right)^{\cdot} - \frac{2}{3}\frac{k^4}{a^4}\delta\pi = 0$

Chapter 3

Assumptions

In order to interpret at all the observations, it is necessary to make some assumptions about the Universe's energy content and geometry. As it should be expected, the level of assumptions determines the observability of some of its properties, or configurations. We would like to refrain from any assumptions that would directly involve a dark energy model. Although, at some level, even the very simple assumption that the Equivalence Principle holds somewhat constrains the possible classes of dark energy models, as we discuss further in more detail.

In order to develop our analysis we base on only, fairly mild, five assumptions:

1. The geometry of the Universe is well described by scalar linear perturbations in a Friedmann-Lemaître-Robertson-Walker metric with scale factor $a(t)$, Eq(2.0.1).

2. We will not consider possible observations of rotational perturbation modes nor of gravitational waves, as these are irrelevant for structure formation in late-time cosmology. We mostly neglect spatial curvature, but since it is observable, its existence would not change our main results. The parameter Ω_{k0} would enter some of the equations, but given how small it is seems to be, it would not affect them in any significant way.

3. The matter content is pressureless. We do not differentiate between dark matter and baryons. We neglect the radiation component because all the observations are assumed to be performed well after decoupling.

4. We assume that the Equivalence Principle holds and therefore that both dark matter and galaxies follow geodesics of the same metric. This allows us to assume that there is no velocity bias between both components.

5. The galaxy distribution is related to the matter distribution through a potentially time-

and scale-dependent linear bias, $\delta_{\rm gal} = b(k,a)\delta_{\rm m}$. We make no assumption about any particular form of the bias function.

6. The late-time Universe is effectively described by the action

$$S = \int \mathrm{d}^4x\sqrt{-g}\left(\tfrac{1}{2}R + \mathcal{L}_x + \mathcal{L}_{\rm m}\right) , \tag{3.0.1}$$

(setting $8\pi G_{\rm N} = 1$) which includes the Einstein-Hilbert term for the metric $g_{\mu\nu}$ and the Lagrangian $\mathcal{L}_{\rm m}$ describing pressureless matter fluids, *both* baryons and dark matter. Any other terms are ascribed to the DE Lagrangian $\mathcal{L}_x$, which is some consistent theory[1] potentially depending on extra degrees of freedom or $g_{\mu\nu}$ (i.e. modifications of gravity). In non-minimally coupled models, the Lagrangian $\mathcal{L}_{\rm m}$ depends on a different metric, related to $g_{\mu\nu}$ through some transformation. Here we assume, however, that we have already reformulated the action so that matter moves on the geodesics of $g_{\mu\nu}$.

We completely ignore the practical problems and limitations of the observations and assume that good-enough statistics with sufficiently small systematic errors can be achieved in the range of redshifts and scales discussed here for, e.g. supernova luminosities, the distribution of galaxies, baryon acoustic oscillation measurements and weak lensing shear. By exploring this idealized case we try to discover the fundamental limits to which observations in a dark energy cosmology are subject.

[1] A consistent theory is here understood to be a theory free of ghost and other catastrophic instabilities that can in general occur in generalized gravity and dark energy models.

Chapter 4

What can be observed

4.1 Background Observables

From assumptions 1-3, by varying the action Eq.(3.0.1) with respect to the metric, we obtain, at zeroth order, a Friedmann equation that can be written as

$$H^2 - H_0^2 \Omega_{k0} a^{-2} = \frac{1}{3}(\rho_x + \rho_{\rm m})\,, \tag{4.1.1}$$

where $H \equiv \frac{\dot{a}}{a}$ is the Hubble parameter and H_0, its present value; Ω_{k0} the present curvature density parameter and $\rho_{\rm m}$ is the matter energy density. From assumption 2, $\rho_{\rm m}$ evolves as a^{-3}, and ρ_x is the energy density of the terms coming from $\mathcal{L}_x$.

Observations of the cosmic expansion assume the existence of standard candles, rods or clocks, which are supposedly known phenomena, in order to make estimations of the luminosity distance $D_L(z)$ of objects. By using assumption 1, i.e. that gravity is a metric theory, whose background is FLRW, one can relate the luminosity distance with the energy content of the Universe:

$$D_L(z) = (1+z)\chi(z), \tag{4.1.2}$$

where $\chi(z)$ is the comoving distance defined as

$$\chi(z) \equiv \frac{1}{H_0}\int_0^z \frac{dz'}{E(z)}, \tag{4.1.3}$$

for a flat Universe, where we also define the dimensionless Hubble function

$$E(z) \equiv H(z)/H_{0.} \tag{4.1.4}$$

The Hubble parameter $H(z)$ can be measured up to a multiplicative constant related to the unknown absolute value of some property of the source, like the total luminosity, or proper length. Let us describe how this information ca be extracted in two important probes, the Supernovae Ia and the acoustic oscillations in the baryon-photon fluid.

Type Ia Supernovae

Luminosity distances from Supernovae are inferred through the observed luminosity L_0 of an object with intrinsic luminosity L, where this intrinsic value is supposed to be a known quantity. From the definition of the flux

$$\mathcal{F} \equiv \frac{L}{4\pi D_L(z)^2} = \frac{L_0}{4\pi \chi(z)^2}, \tag{4.1.5}$$

one can relate the intrinsic and the observed luminosities. And by expanding the comoving distance (4.1.3) up to small redshift values, one gets $\chi(z) \simeq \frac{z}{H_0}$. So we can write the luminosity distance as

$$D_L(z) \simeq z/H_0.$$

.

Thus, the flux of type Ia Supernovae is known up to the constant LH_0^2 and only ratios of fluxes at different redshifts are independent of the absolute normalization [4].

Baryon acoustic oscillations

Another important probe of smooth quantities comes from the baryon acoustic oscillations (BAO). Baryons, electrons and photons were coupled through Coulomb and Compton interaction as a single fluid until recombination. Radiation pressure resists the gravitational compression into the potential wells, causing the baryon-photon fluid to oscillate. During the recombination, the Compton scattering rate between electrons and photons lows down releasing the baryons from the photons drag, this happens at redshift of ~ 1020, and it is called drag epoch. We want to call the attention for the fact that the decoupling between baryons and photons is different from the decoupling between photons and electrons that happens latter on releasing the CMB photons at redshift ~ 1100. The fact that we can predict the ratio of baryons to photons density makes the oscillations on the baryon-photon fluid prior to decoupling an additional standard ruler. That's because the peaks and troughs patterns in the fluid leave a mark on the matter power spectrum. The positions of these peaks and troughs depend on the sound horizon, and the sound horizon is determined by the ratio of baryon to photon [4, 34, 35].

In order to extract information on background quantities from BAO, let us first define the angular diameter distance from an object of intrinsic size s that subtends and angle $\Delta\theta$.

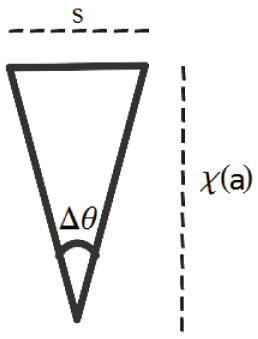

Figure 4.1.1: Angular diameter distance

If this object is at a comoving distance $\chi(a)$, this relates to the angular diameter distance as $D_A = \chi(a)\, a$, and we get

$$\triangle\theta \equiv \frac{s}{\chi(a)} = \frac{s\, a}{D_A}. \tag{4.1.6}$$

For BAO, the observed object is the sound horizon at which baryons were released from the photon drag, defined by

$$r_s(z_{drag}) \equiv \int_0^{\eta_{drag}} c_s(\eta), \tag{4.1.7}$$

η here is the conformal time $\eta = \int \frac{dt}{a}$ and the sound speed is given by the ratio of the pressure and energy density perturbation of the fluid

$$c_s \equiv \frac{\delta P_\gamma}{\delta\rho_\gamma + \delta\rho_b} = \frac{4\rho_\gamma}{3\,(4\rho_\gamma + 3\rho_b)}. \tag{4.1.8}$$

Therefore BAO allows us to measure the following ratios, up to the size of the sound horizon.

$$\begin{aligned} \triangle\theta &= \frac{r_s\, a}{D_A}, \\ \delta z &= r_s\, H(z). \end{aligned} \tag{4.1.9}$$

From real-time redshift drift [**?**], one can also determine the absolute value of the Hubble parameter, while local measurements of H_0. Summing up, background observables are $D_L(z)$,

$D_A(z)$ up to an overall constant and the dimensionless Hubble function $E(z) \equiv H(z)/H_0$. Moreover, because the luminosity distances depend on the present curvature parameter Ω_{k0}, we can combine $D_L(z)$ and $E(z)$ to estimate this quantity.

We can therefore determine the evolution of the combined matter and dark energy content, $1 - \Omega_k$, at all times. If we assume that there are only two components of the cosmic fluid then we have only one free parameter, $\Omega_{\rm m0}$. In fact we can write

$$\Omega_x = 1 - \Omega_k - \Omega_{\rm m} = 1 - \frac{1}{E^2}\left(\Omega_{k0}a^{-2} + \Omega_{\rm m0}a^{-3}\right) . \tag{4.1.10}$$

From the above, we conclude that from background observables we can reconstruct both $\Omega_{\rm m}$ and Ω_x, but only up to $\Omega_{\rm m0}$ [36], since one can compensate for any change of $\Omega_{\rm m0}$ with a modification of the DE model. Of course, if we parametrize the evolution of Ω_x with a simple equation of state, we can break the degeneracy with $\Omega_{\rm m0}$, as is usually done in analysis of SNIa data, but that is exactly what we are trying to avoid in our approach.

The same result is valid if instead of pure pressureless matter one includes further components (e.g. massive neutrinos) that evolve with an effective equation of state $w_{\rm m}(z)$, provided $w_{\rm m}(z)$ can be inferred from other observations (e.g. knowledge of the neutrino masses).

4.2 Linear Perturbations Observables

At the linear level, the observables are correlations in angular separation and redshift of positions, velocities and shapes of sources, i.e. galaxies, clusters of galaxies, Lyman-α lines and the Cosmic Microwave Background. The knowledge about the the luminosity distance of these correlations can be converted to the wavenumber k_{phys} and redshift. When discussing linear perturbations, we denote with perturbation variables (e.g. Φ, Ψ, δ_{gal}, etc.) the square root of their power spectrum, as is common in the literature. These are therefore positive-definite quantities and their ratio is well defined.

4.2.1 Matter clustering and Redshift-space distortions

We can observe galaxies, not matter perturbations. Assuming that galaxies fall into the gravitational potential of dark matter, tracing the DM perturbations, we can relate both components through a scale and time-dependent bias $b(k, a)$, such that

$$\delta_{gal} = b(k, a)\delta_m. \tag{4.2.1}$$

Moreover, galaxies are observed not in real space, but in redshift space. The quantity

we observe is the perturbed galaxy number density, and it is affected by perturbations on the redshift positions of the galaxies and the space volume. These effects can be generally characterized by the peculiar velocity of the galaxies and metric potentials[1]. In fact, the nomenclature, redshift-space distortion (RSD) traditionally refers to the peculiar motions only, and other corrections have been taken into account only recently. In simulations for a ΛCDM fiducial model [37], it was shown that redshift space distortions due to peculiar velocities are the dominant correction to the number density. In our work, we shall restrict to this effect as a first approximation (and refer to it as RSD), in a second phase, we wish to evaluate other corrections more closely.

By taking into account the corrections to the galaxies redshift in a systematic way, one can extract the correction to the galaxy number density. Traditionally one uses the velocity of the galaxy field to extract information about the underlying dark matter distribution through a bias, and relates the redshift-space distortion (RSD) to the dark matter growth rate [2] [38]:

$$\delta^z_{\rm gal}(k,z,\mu) = b\left(1+\frac{f}{b}\mu^2\right)\delta_m(k)\,. \tag{4.2.2}$$

where the growth rate of dark matter perturbations is described as

$$f(k,a) \equiv \delta'_m(k,a)/\delta_m(k,a). \tag{4.2.3}$$

This connection with matter perturbations through an unknown bias is, however, not necessary for our purposes, as we discuss below. Fundamentally, the Kaiser formula, Eq(4.2.4) for the redshift-space galaxy number density $\delta^z_{\rm gal}$ is a statement about a correction to the real-space galaxy number density $\delta_{\rm gal}$ resulting from the peculiar velocities of the galaxies [39],

$$\delta^z_{\rm gal}(k,z,\mu) = \delta_{\rm gal}(k,z) - \mu^2\frac{\theta_{\rm gal}(k,z)}{H}\,, \tag{4.2.4}$$

where $\theta_{\rm gal}\equiv \nabla^i v_i$, is the velocity divergence and μ, the direction cosine. This means RSD potentially constitutes a measurement of $\theta_{\rm gal}(k,z)$, at different redshifts and scales. Now, rather than relating this velocity to dark matter evolution, we can make a choice that allows us to avoid any assumption about the velocity bias: galaxies move on geodesics of the metric, whatever the actual source of this metric

$$\left(a^2\theta_{\rm gal}\right)' = a^2 H k^2 \Psi\,, \tag{4.2.5}$$

[1] These were fully addressed in [37] where the authors simulated the transverse power spectrum for a ΛCDM model and calculated the corrections to $\delta_{gal}(k,a)$ for different redshifts and scales.

[2] See e.g. [38, 39]. This is how we proceeded in Ref. [29].

with $k \equiv k_{\rm com}/aH$. We can now integrate Eq(4.2.5), neglecting the integration constant, to discover that from the angular dependence of the two-dimensional galaxy power spectrum we can extract the following two observables, that we acknowledge as

$$A = \delta_{\rm gal}\,, \quad R = -\frac{\theta_{\rm gal}}{H} = -\left(a^2 H\right)^{-1} \int a^2 H k^2 \Psi \mathrm{d}\ln a\,.$$

This approach allows us to see that linear RSD are really a measurement of the gravitational potential Ψ which accelerates the galaxies

$$-k^2\Psi = R' + R\left(2 + \frac{E'}{E}\right)\,. \tag{4.2.6}$$

In addition to this, if we simply evoke the Equivalence Principle, i.e. galaxies and dark matter follow the same geodesics, the observation of $\theta_{\rm gal}$ implies the observation of θ_m. In other words, there is no velocity bias and $\theta_{gal} = \theta_m$. Notice that, without this assumption about the velocity bias, we would not be able to reach this conclusion. On the other side, in the case of matter perturbations, because we have not made any assumptions about the bias, it was not possible to infer knowledge about δ_m from δ_{gal}.

Considering the measurement of θ_m, from the continuity equation

$$\delta'_{\rm m} + H^{-1}\theta_{\rm m} = -3\Phi'\,, \tag{4.2.7}$$

we see that, if time-derivatives of the potential are not varying rapidly in the scales of interest, i.e. in some quasi-static regime, the continuity equation approximates to $\delta'_{\rm m} + H^{-1}\theta_{\rm m} \simeq 0$, meaning we end up with a measurement of $\delta'_{\rm m}$.

Statistical origins of the velocity bias a part [40], there could in principle be a non-vanishing bias between these two velocities. Indeed, this happens in any model in which there is a fifth force acting on dark matter, which does not couple to baryons or light, i.e. models with a violation of the Equivalence Principle such as coupled quintessence [41]. This fifth force is a new source of acceleration for dark-matter particles, causing their peculiar velocities to deviate from that of the galaxies. The effect of this is to introduce a (scale and time-dependent!) velocity bias.

In principle, one could also directly measure the galaxies velocities. The estimation of it requiring a subtraction of the peculiar redshift from the cosmological redshift by using distance indicators such as Cepheids and therefore a number of additional assumptions on the source physics. No current or foreseeable method to estimate the peculiar velocity field has been shown to be reliable beyond a few hundred megaparsecs (see e.g. [42]), so we will not pursue this possibility any further.

4.2.2 Weak gravitational lensing

Weak gravitational lensing is a probe of the distortion in the path of photons emitted from galaxies due to the lensing potential along the line of sight. The observed shape of the galaxies is deformed by a very small amount, but it is possible to quantify this effect through statistics of a large number of galaxies.

Usually, the lensing caused by the potential is used as a tracer of the matter content that sources the potential. To our purposes, we would simply like to extract the information about the potential itself. More explicitly, weak lensing is sensitive to the projection of the lensing potential along the line of sight [43], defined as the convergence

$$\mathcal{C} = \frac{1}{2}\int_0^{D_{As}} k^2(\Psi - \Phi) g(D_A, D_{As}) dD_A, \tag{4.2.8}$$

where D_A and D_{As} are the angular diameter distances of the lens and the source, respectively, and $g(D_A)$ is a window function that basically gives the efficiency with which the gravitational potential lens a given normalized galaxy distribution $W(\chi)$. And it described by

$$g(\chi) = \chi(D_A)\int_{D_A}^{D_{A0}} \frac{r(D'_A - D_A)}{r(D'_A)} W(D'_A) dD'_A, \tag{4.2.9}$$

where $\chi(z)$ is the comoving angular distance and D_{A0} is the horizon angular diameter distance.

Through integral 4.2.8 one sees that, in principle, it is possible to extract the lensing potential as a function of redshift (conversely, a) and scale k, provided we have data with the required precision at a range of scales and redshifts.

$$[\Psi - \Phi](k, a). \tag{4.2.10}$$

We can, therefore, define the following observable quantity

$$L \equiv (\Psi - \Phi) E^2 a^3 k^2, \tag{4.2.11}$$

where the term $E^2 a^3 k^2$ does not change our conclusions, and facilitates the connection with the usual notation discussed in section 4.4.

Summarizing the above, by combining redshift-space distortions and weak lensing, we are able to reconstruct the Jordan-frame metric for galaxies and light. However, those probes provide no information about the Jordan frame of the underlying dark matter. In principle, one could use different tracers with different baryon fractions (cluster and galaxy power spectra) to map out the Jordan frames for these two classes of objects and obtain some

information on the differences in the gravitational potentials they experience (in the spirit of e.g. [44]). Interestingly, galaxies are not just baryons, but are dynamically coupled to their dark-matter halos. This means that the Jordan-frame metric for the galaxies is not necessarily the same as the one for baryons, since the galaxies will at least partly feel the fifth force acting on dark-matter. In this case, measurements of WL and RSD would still reconstruct the same metric potentials for our tracers, but these are not the complete potentials that the dark matter feels. Allowing for such deviations, we completely loose the connection between the dark matter growth rate and RSD of the galaxy power spectrum.

Let us summarize this section with the following scheme:

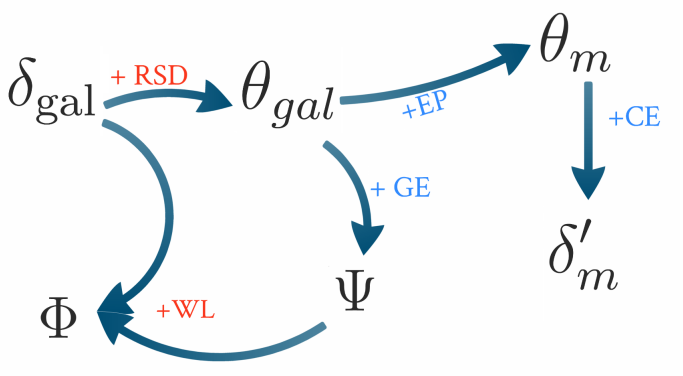

Figure 4.2.1:
Linear perturbation observable quantities: In red, we identify the probes and in blue, the theoretical assumption that must hold in order to identify the observables.

4.3 Dark energy configuration

Having identified which quantities are observables without assuming a model for dark energy, we would like to turn to how these quantities relate to a general dark energy configuration.

It has been argued [45, 46] that there are two quantities that are, in principle, capable of fully relating observations to a particular dark energy model. They are the slip parameter (or anisotropic stress) and the effective gravitational coupling, defined respectively as

$$\eta(k,z) \equiv -\Phi/\Psi\,, \qquad Y(k,z) \equiv -\frac{2k^2\Psi}{3\Omega_{\rm m}\delta_{\rm m}}\,, \tag{4.3.1}$$

The idea is that there are four fields that fully describe the scalar perturbations: $\{\delta_m, v, \Phi, \Psi\}$. We can provide two equations for the matter component, i.e. the covariant conservation of the energy momentum tensor

$$E_v \equiv \left(a^2\theta\right)' = a^2 H k^2 \Psi\,, \tag{4.3.2}$$

$$E_\delta \equiv \delta'_{\rm m} + H^{-1}\theta_{\rm m} = -3\Phi' \,. \tag{4.3.3}$$

Therefore, by introducing the two parameters Y and η from a specific DE model, one can, in principle, describe the evolution of matter perturbations and hope to connect them to the observed structure formation.

However, when considering a dark energy model, one sees that it is not simple to obtain a separate form for Y and η . In fact, in many DE models, they are described by a set of differential equations and it is impossible to obtain an algebraic, separate form for them. The usual approach in this case consists on parametrizing these quantities. In the ΛCDM model, for instance, they are both parametrized to be $Y = 1$ and $\eta = 1$.

Another example of parametrization, appears when the quasi-static limit of some theory is taken. Many authors argue that the gravitational potentials and the scalar-field oscillations can be safely neglected in scalar-tensor theories, as they do not oscillate very fast.

Considering this limit, for instance in the Horndeski theory (the most general scalar-tensor theory), all time derivatives of the potentials and the perturbed scalar are dropped, therefore all time derivatives of Y and η are also dropped (except for a factor proportional to the growth rate $f(k, a)$, that comes from Y'). These ratios are then drastically simplified, making it possible to write them in a simple time- and scale-dependent form, where both quantities depend only on a small number of parameters that connects them to the Lagrangian

$$Y = h_1 \left(\frac{1 + k^2 h_5}{1 + k^2 h_3}\right) , \quad \eta = h_2 \left(\frac{1 + k^2 h_4}{1 + k^2 h_5}\right) , \tag{4.3.4}$$

where h_i are time-dependent background quantities which forms are not relevant for the moment.

As will become clear along this thesis, our approach in [29, 31] differs sensibly from the standard one, where parametrized functions are introduced in a modified code that will evolve them while simultaneously fitting the data in a model- (parametrization-) dependent way. Our proposal consists in firstly elucidating which quantities are observables *a priori* and, then using this information to directly constrain data, by simply measuring these observables at different redshifts and scales, not requiring any parametrization, or even the quasi-static assumptions.

An important conclusion of our analysis is that the anisotropic stress η is directly observable, for it constitutes a ratio of the metric potentials, that we have shown to be observables. On the other hand, the gravitational coupling Y is *not* an observable quantity, for it depends on the value of δ_m, which is *not* observable. Another important quantity used to describe perturbations is the linear matter growth $f(k, a) \equiv \frac{\delta'_{\rm m}}{\delta_{\rm m}}$, that similarly to Y does not constitute

and observable.

Let us introduce some ratios that will prove useful in chapter 6, when we will use the observable quantities to constrain dark energy models:

$$\Gamma \equiv \frac{\Psi'}{\Psi} = \frac{L'}{L} - \frac{\eta'}{1+\eta} - 1\,, \qquad (4.3.5)$$
$$\frac{\Phi'}{\Phi} = \Gamma + \frac{\eta'}{\eta} = \frac{L'}{L} + \frac{\eta'}{\eta\,(1+\eta)} - 1\,,$$

where L is the observable defined in Eq(4.2.11).

In the next section we will describe how the dar)k energy configuration relates to the dark matter properties, identifying which quantities related to dark matter are observable. This will put our ignorance about the dark sector in evidence and will show how our knowledge is limited to combinations of quantities, that alone, are not observables. In spite of this ignorance, in section 5, we will work out some consistency relations between observable and unobservable quantities that will constitute a consistency check to be applied to observations.

4.4 Connection to dark matter

In the previous section, we have somewhat deviated from the standard approach, that is to try to reconstruct dark matter perturbations from weak lensing and redshift-space distortions. Our attempt was to make a more agnostic path, avoiding to deal with bias and the dark matter perturbation itself, for they are not measurable. In this section we will follow the standard path relating the probes with the dark matter. As dark matter perturbations are not observable, we will present observable combinations of quantities that relate to the DM properties.

4.4.1 Matter clustering

We can observe galaxies. One of our assumptions is that galaxies trace dark matter perturbations through an unknown linear bias, generally described by a scale- and time-dependence: $\delta_{\rm gal}(k,a) = b(k,a)\delta_m(k,a)$. We now define the growth function $G(k,a)$ for matter perturbations through

$$\delta_{\rm m}(k,a) \equiv G(k,a)\delta_{\rm m}(k,a_0) \qquad (4.4.1)$$

where we have emphasized the scale and time-dependence of the quantities, but from now on, we will often omit the parenthesis, when convenient, and use, e.g. $\delta_{\rm m}(k, a_0) \equiv \delta_{\rm m,0}$.

So our first observable can be expressed as [3]

$$A \equiv \delta_{\rm gal} = Gb\delta_{\rm m,0}. \tag{4.4.2}$$

4.4.2 Redshift-space Distortion

As we discussed in section 4.2, from the statistical analysis of the anisotropy of galaxy clustering we can infer the redshift-space distortions caused by the peculiar velocities of galaxies

$$\delta^z_{\rm gal}(k, a, \mu) = \delta_{\rm gal}(k, a) - \mu^2 \frac{\theta_{\rm gal}(k, a)}{H}\,, \tag{4.4.3}$$

which, in sub-Hubble scales, in the case where the field slowly oscillates, allows us to approximate $\theta_{\rm gal} = \theta_{\rm m} \simeq -\delta'_{\rm m} = -f\delta_{\rm m}$, and the RSD effect can be expressed in the traditional Kaiser formula [38]

$$\delta^z_{\rm gal}(k, a, \mu) = b\left(1 + \frac{f}{b}\mu^2\right)\delta_m(k, a)\,. \tag{4.4.4}$$

With this approximation, we can express the observable R in terms of the initial matter density perturbation, defining our second observable quantity in terms of the the following combination:

$$R = -\frac{\theta_{\rm gal}}{H} \simeq \delta'_m = Gf\delta_{\rm m,0}\,, \tag{4.4.5}$$

where G was previously defined in Eq (4.4.1), and f is the matter linear growth rate, define in Eq(4.2.3).

[3] Notice that in [29] we have used the notation $\delta_{\rm m,0} = \sigma_8\delta_{\rm t,0}$, taking into account the total density perturbation, including that of dark energy. In this paper, we wanted to stress one of the discussions of this thesis, i.e. that there is an unknown distribution of dark energy perturbations which affects gravitational measurements. In this section we solely want to discuss how observables relate to the dark matter properties, therefore we focus on $\delta_{\rm m,0}$.

4.4.3 Weak Lensing

In the linear regime, the lensing effect is proportional to the lensing potential, which itself is driven by the density perturbations (see e.g. [12]). In general, this relation can be written as

$$k^2(\Psi - \Phi) = -\frac{3}{2} Y(1+\eta)\Omega_{\rm m}\delta_{\rm m} \tag{4.4.6}$$

$$= \frac{1}{E^2 a^3}\Omega_{\rm m0} G Y(1+\eta)\delta_{\rm m,0} \tag{4.4.7}$$

where, from the Friedmann equation, we have used that

$$\frac{\Omega_{\rm m}}{\Omega_{\rm m0}} = \frac{1}{E^2 a^3}, \tag{4.4.8}$$

and therefore, we can define our third observable, corresponding to the lensing potential as the combination

$$L = \Omega_{\rm m0} G Y(1+\eta)\delta_{\rm m,0}. \tag{4.4.9}$$

So, the observable combinations of quantities that relates to dark matter perturbations are.

$$A = Gb\delta_{\rm m,0}\,, \quad R = Gf\delta_{\rm m,0}\,, \tag{4.4.10}$$

$$L = \Omega_{\rm m0} Y(1+\eta) G\delta_{\rm m,0}\,. \tag{4.4.11}$$

Now, let us remark that the amplitude of the density perturbation today $\delta_{\rm m,0}$ depends on the whole history of the common evolution of the unknown dark energy and dark matter, and the initial conditions in both these components. For instance, the Cosmic Microwave Background anisotropy allows one to measure, at least in principle, the initial total lensing potential $[\Psi - \Phi]_{\rm in}$ through the Sachs-Wolfe effect. However, it is impossible to derive the present power spectrum from this information. The present power spectrum depends, in fact, on a scale- and time-dependent transfer function, that acts to process the total perturbation spectrum, changing its $k-$dependence and that, without further assumptions, i.e. absent a model for DE, remains unknown. Thus, the conclusion from the list (4.4.10) of observable combinations is that it is impossible to measure $\delta_{\rm m,0}$ without a knowledge of the bias b.

As a consequence, only the ratios of A, R, L, and their N-derivatives, are directly measurable from linear cosmological observations, being $\delta_{m,0}$-independent quantities

$$P_1 \equiv \frac{R}{A} = \frac{f}{b}, \tag{4.4.12}$$

$$P_2 \equiv \frac{L}{R} = \frac{\Omega_{\rm m0} Y (1+\eta)}{f}, \tag{4.4.13}$$

$$P_3 \equiv \frac{R'}{R} = f + \frac{f'}{f}. \tag{4.4.14}$$

All other possible $\delta_{\rm m,0}$-independent ratios, such as A'/A, L'/L or R'/L or higher-order N-derivatives, can be obtained as combinations of P_{1-3} and their derivatives.

We will refer to the observables P_i as the primary model-independent observables. The observable P_1 contains the bias that, as we already discussed, cannot be measured in a model-independent manner and therefore we will not use it any further in our discussion. The observable P_2 has already been introduced in [43] as E_G as a test of modified gravity, but the fact that $\Omega_{\rm m0}$ is not an observable was not discussed there.

We should emphasize that these results, for example from the form of $P_{3,}$, imply that the growth rate of dark matter f, cannot be measured without picking a particular model or at least a parametrization for dark energy, since the equation $f'/f + f = P_3(k,a)$ cannot be solved without the unknown k-dependent initial condition for f.

The quantity $R \equiv Gf\delta_{\rm m,0} = Gf\sigma_8\delta_{\rm t,0}$ contains the combination $Gf\sigma_8(z)$, often denoted as $f\sigma_8(z)$ in the literature [47], which is considered to be a directly observable quantity. However, this is of course true only if one assumes a model for DE, or at least a parametrized form of $\delta_{t,0}$; otherwise, the model-independent observable combination is $P_3 = R'/R$. It is important to realize that even a perfect knowledge of P_3 does not imply knowledge of f since the equation $f'/f + f = P_3(k,z)$ cannot be solved without the unknown k-dependent initial condition for f. Finally, notice that we did not need to assume Gaussian fluctuations nor isotropy of the power spectrum.

In table (5.1), we summarize all the variables presented in this section.

Chapter 5

Consistency Relations

It is useful to notice how observables can be related and this could provide us with some consistency tests. Here we present how we have arrived at such consistency relations.

5.1 First Consistency Relation: the observability of η

We firstly consider the equation for the evolution of matter perturbations in the subhorizon regime. This is obtained by taking the subhorizon limit of the second conservation equation for matter, Eq(4.3.3)

$$\theta_{\rm m} \simeq -H\delta'_{\rm m}\,, \tag{5.1.1}$$

and replacing it in the first conservation equation Eq(4.3.2), resulting

$$\delta''_{\rm m} + \left(2 + \frac{H'}{H}\right)\delta'_{\rm m} = -k^2\Psi. \tag{5.1.2}$$

Now, in order to see the connection with the primary observables P_i, we rewrite this equation in terms of the growth function:

$$f' + f^2 + \left(2 + \frac{H'}{H}\right) f = -k^2\Psi. \tag{5.1.3}$$

Dividing the above by f, we immediately recognize the observable $P_3 \equiv f + \frac{f'}{f}$, on the left-hand-side, and $P_2 \equiv \frac{\Omega_{\rm m0}Y(1+\eta)}{f} = -\frac{2}{3}\Omega_{\rm m0}\frac{k^2\Psi(1+\eta)}{\Omega_{\rm m}\delta_{\rm m}}\frac{\delta_{\rm m}}{\delta'_{\rm m}}$, on the right-hand-side, thus giving the follow relation

$$\frac{3P_2(1+z)^3}{2E^2\left(P_3+2+\frac{E'}{E}\right)}-1=\eta\,, \tag{5.1.4}$$

where we have again, used that $\frac{\Omega_{\rm m}}{\Omega_{\rm m0}}=\frac{(1+z)^3}{E^2}$, and $E=H(z)/H_0$.

We have called this result a consistency check [29], because the observed form of the anisotropic stress, potentially scale-dependent in a general dark energy model, can be tested for. Equation (5.1.4) is however, more than just a consistency test, it states the observability of η, as we have already demonstrated through a different path in sections4.2 and 4.3, by considering the observability of the metric potentials.

5.2 Consistency Relation for Y

In a completely independent way, we work out relations between observables and the effective gravitational coupling. By taking the time derivative of P_2 we find

$$\frac{P_2'}{P_2}=-\frac{f'}{f}+\frac{Y'}{Y}+\frac{\eta'}{1+\eta}\,. \tag{5.2.1}$$

Now we use that

$$\frac{f'}{f}=P_3-f=P_3-\frac{\Omega_{\rm m0}Y(1+\eta)}{P_2}\,, \tag{5.2.2}$$

and rearrange some terms, so Eq(5.2.1) results

$$\frac{P_2'}{P_2}+P_3-\frac{\eta'}{1+\eta}=\frac{\Omega_{\rm m0}Y(1+\eta)}{P_2}+\frac{Y'}{Y}\,. \tag{5.2.3}$$

Already here, one can see that the left-hand-side consists exclusively of observable quantities, while the right-hand-side has the quantity Y, that we are not able to determine, unless we provide some initial condition. It is interesting to note that the combination $\frac{\eta'}{1+\eta}$ can be written as

$$\frac{\eta'}{1+\eta}=\frac{P_2'}{P_2}-\frac{\left((\frac{E'}{E})^2+P_3'+\left(2(2+P_3)\frac{E'}{E}+\frac{E''}{E}\right)\right)}{\left(2+P_3+\frac{E'}{E}\right)}, \tag{5.2.4}$$

and from Eq(5.1.4), we define the observable quantity

$$\varpi\equiv\frac{\eta+1}{P_2}=\frac{2E^2\left(P_3+2+\frac{E'}{E}\right)}{3(1+z)^3}. \tag{5.2.5}$$

Thus, combining Eq.(5.2.3), Eq.(5.2.4) and Eq.(5.2.5), one can write a consistency relation that depends only on the observation of P_3 :

$$\frac{Y'}{Y}+\frac{3(1+z)^3\Omega_{m0}Y}{2E^2\left(2+P_3+\frac{E'}{E}\right)}=\frac{\left(2E^2\left(2+P_3+\frac{E'}{E}\right)\right)'+2P_3E^2\left(2+P_3+\frac{E'}{E}\right)}{2E^2\left(2+P_3+\frac{E'}{E}\right)}.$$

Now, remember that P_3 is defined to be $\frac{R'}{R}$, so the consistency check depends only on the observability of R, that corresponds to what one can probe through redshift-space distortions: the Newtonian potential Ψ(see Eq(4.2.6)). This actually could have saved us a lot of work. In the end, this same consistency check can be simply expressed as

$$\frac{Y'}{Y}+\Omega_{\rm m0}\varpi Y=1+\Gamma\,. \tag{5.2.6}$$

where we have used the observables defined in Eq.(4.3.5): $\Gamma\equiv\frac{\Psi'}{\Psi}$ and in Eq.(5.2.5) :$\varpi\equiv\frac{\eta+1}{P_2}$ that one can easily obtain by using the definition of Y and the relation between f and P_2.

The consistency relation for Y expresses our incapacity to determine its value through observations. It constitutes a first-order differential equation for the combination $\Omega_{\rm m0}Y$, that without the choice of some initial condition, we are not able to solve. As we will discuss further, this is a result of the dark degeneracy in the perturbative level, and the initial condition to furnish with, is exactly the initial value of the dark matter perturbations.

Class	Variable	Key Relation	Obs.?	Eq.	Comment
Measurements	A	$\equiv \delta_{\rm gal} = b\delta_{\rm m}$	✓	(4.4.2)	Bias not measurable absent DE model
	R	$\equiv -\theta_{\rm gal}/H$	✓	(4.4.5)	RSD measure galaxy velocity
	L	$\equiv \frac{2k^2E^2}{3(1+z)^3}(\Phi - \Psi)$	✓	(4.4.9)	WL shear probes lensing potential
	E	$\equiv H/H_0$	✓	(4.1.4)	H_0, $\Omega_{\rm m0}$ not observable without DE model
Primary	$P_1 = \beta$	$\equiv R/A = f/b$	✓	(4.4.12)	
observables	$P_2 = E_G$	$\equiv L/R = (1+\eta)/\varpi$	✓	(4.4.13)	
	P_3	$\equiv R'/R = f + f'/f$	✓	(4.4.14)	Only this function of f is observable
Physical	Ψ	$R' + R\,(2 + {}^{E'}/_{E})$	✓	(4.2.6)	Extract from RSD
variables	Φ	$\frac{3(1+z)^3}{2k^2E^2}L + \Psi$	✓		Extract from WL tomography
	$\delta_{\rm m}$	$\delta_{\rm m} = \delta_{\rm gal}/b$			Unknown without knowing bias
	$\theta_{\rm m}/H_0$	$\theta_{\rm m} = \theta_{\rm gal}$	✓		Observable only given Equivalence Principle
DE	η	$\equiv -\Phi/\Psi$	✓	(4.3.1)	$\eta \neq 1 \Rightarrow$ coupling DE/gravity
Configuration	Γ	$\equiv \Psi'/\Psi$	✓	(4.3.5)	Observable prediction of DE models
Variables	Y	$\equiv -2k^2\Psi/3\Omega_{\rm m}\delta_{\rm m}$		(4.3.1)	$\delta_{\rm m}$ unknown; must satisfy relation (5.2.6)
	f	$\equiv \delta'_{\rm m}/\delta_{\rm m}$		(4.3.1)	$\delta_{\rm m}$ unknown
	ϖ	$\equiv f/\Omega_{\rm m0}Y$	✓	(5.2.5)	Relates DM velocity to potential

Table 5.1: Summary of variables used in Part I of the thesis. Those variables marked with a checkmark as observable can be measured as a function of redshift and scale without an assumption of a particular DE model. Measurement of $\delta_{\rm m}$ requires the knowledge of bias, which cannot be measured or modeled without the knowledge of the DE model. The variables such as Y and f typically used to describe the DE configuration are therefore not observable, but predictions can be reformulated to maximally exploit those variables which are observable (see section 6.3).

Chapter 6

The Horndeski Lagrangian

The most general second-order scalar-tensor theory is described by the Horndeski Lagrangian (HL) [48, 49][1]. The HL is defined as the sum of four terms $\mathcal{L}_2$ to $\mathcal{L}_5$ that are fully specified by a non-canonical kinetic term $K(\phi, X)$ and three in principle arbitrary coupling functions $G_{3,4,5}(\phi, X)$, where $X = -g_{\mu\nu}\phi^{,\mu}\phi^{,\nu}/2$ is the canonical kinetic term,

$$\begin{aligned}
\mathcal{L}_2 =& K(\phi, X)\,, \\
\mathcal{L}_3 =& -G_3(\phi, X)\Box\phi\,, \\
\mathcal{L}_4 =& G_4(\phi, X)R + G_{4,X}\left[(\Box\phi)^2 - (\nabla_\mu\nabla_\nu\phi)^2\right]\,, \\
\mathcal{L}_5 =& G_5(\phi, X)G_{\mu\nu}\nabla^\mu\nabla^\nu\phi - \frac{G_{5,X}}{6}\Big[(\Box\phi)^3 - \\
& - 3\,(\Box\phi)\,(\nabla_\mu\nabla_\nu\phi)^2 + 2\,(\nabla_\mu\nabla_\nu\phi)^3\Big]\,.
\end{aligned}$$

In general the equation of motion for the scalar will couple to the matter energy density. The structure of the energy-momentum tensor for the general theory is rather complex, in particular, the Lagrangian features a non-minimal coupling to gravity. This means that the EMTs for any such models will feature, in general, anisotropic stress related to the perturbations of the scalar. The metric potentials Φ and Ψ are as usual determined by the Poisson and anisotropy equations which are constraints and therefore do not have independent dynamics.

The Horndeski Lagrangian encompasses many of the dark energy models proposed in the last decade, e.g. k-essence, Kinetic Gravitational Braiding, Chameleons, Brans-Dicke and $f(R)$. Before addressing the complete theory, we would like to introduce an intermediate analysis, exploring the subclasses of models described by the k-essence Lagrangian, not only for the popularity and importance of this model, but also in order to make a point about the

[1]The equations of motion are second-order for both the scalar and the metric on an arbitrary background

level of constraint we can get for each theory and how this depends on the theory exhibiting non-minimal coupling.

6.1 K-*essence*

Here, we will turn to the simplest class of scalar field models, those described by the Lagrangian $\mathcal{L}_\phi = K(\phi, X)$ [50, 51, 52]. The energy momentum tensor possessed by this kind of dark energy has perfect-fluid form and at linear level all the properties are described by the equation of state w and the sound speed c_s [53]. This example will provide for sufficient complexity in order to demonstrate the logic of our method and the fundamental limitations of constraining the dark energy model space as a result of the non-observability of Y, while having the advantage of being familiar to a wide audience. Note that all uncoupled quintessence models are contained within this class as are perfect-fluid models, provided only scalar perturbations be considered.

We shall not give the full Einstein equations here (their explicit form is in appendix 8.1), but it will suffice to say that the combined k-*essence* and dark matter energy-momentum tensor depends on the perturbation variables schematically as

$$\begin{aligned} \delta T^0_0 &\supset \delta\phi, \dot{\delta\phi}\,, \delta_\mathrm{m} \\ \delta T^0_i &\supset \delta\phi\,, \theta_\mathrm{m} \\ \delta T^i_i &\supset \delta\phi, \dot{\delta\phi}\,, \\ \delta T^i_j - {}^1\!/_3 \delta^i_j \delta T^k_k &= 0\,, \end{aligned} \tag{6.1.1}$$

with $\delta\phi$ the perturbation of the k-*essence* scalar. This model does not allow for any anisotropic stress and therefore it could be immediately excluded if, even at just one redshift and scale, $\eta \neq 1$. We will assume that no such detection was made and therefore we will take $\Phi = -\Psi$. We can then use the combination of the Hamiltonian and momentum constraints [i.e. the (00) and ($0i$) Einstein equations], to eliminate the scalar-field perturbations $\delta\phi$ and $\dot{\delta\phi}$ in the (ii) Einstein equation, obtaining the exact equation for the evolution of the gravitational potential in k-*essence* models in the presence of dark matter

$$\begin{aligned} \Psi'' + \left(4 + \frac{E'}{E} + 3c_\mathrm{a}^2\right)\Psi' + \left(3 + 2\frac{E'}{E} + 3c_\mathrm{a}^2\right)\Psi + \\ + c_\mathrm{s}^2 k^2 \Psi = -\frac{3}{2}\Omega_\mathrm{m}\left(c_\mathrm{s}^2\delta_\mathrm{m} + 3(c_\mathrm{a}^2 - c_\mathrm{s}^2)k^{-2}H^{-1}\theta_\mathrm{m}\right)\,. \end{aligned} \tag{6.1.2}$$

where the adiabatic sound speed,

$$c_{\rm a}^2 \equiv \frac{\dot{p}_X}{\dot{\rho}_X} = -\frac{6{}^{E'}\!/_{E} + 2\left({}^{E'}\!/_{E}\right)^2 + 2{}^{E''}\!/_{E}}{9\Omega_{\rm m0}E^{-2}(1+z)^3 + 6{}^{E'}\!/_{E}}\,,$$

is fully determined by the observable expansion history up to $\Omega_{\rm m0}$. $\theta_{\rm m}$ can be neglected sufficiently deep subhorizon, although this term it is actually observable as $\theta_{\rm m}/H = -R$ and can also be included in the calculation. Equation (6.1.2) is quite standard, see the closely related result in e.g. [54, Eq. 7.51]

Apart from the parameters of this model—the constant $\Omega_{\rm m0}$ and the sound speed $c_{\rm s}$, which can be a function of time—all the quantities on the left-hand-side of Eq. (6.1.2) are observable. What is *not* observable is $\delta_{\rm m}$, as we have explained in section 4.2. Since, at any one redshift slice, the dark-matter configuration can in principle be arbitrary, Eq. (6.1.2) does not by itself provide a constraint on the theory space. However, we can think of Eq. (6.1.2) as a measurement of Y *given the assumption* that the dark energy model belongs to the k-*essence* class:

$$\hat{Y} = \frac{c_{\rm s}^2 k^2}{\left[\Gamma' + \left(\Gamma + 3 + {}^{E'}\!/_{E} + 3c_{\rm a}^2\right)(1+\Gamma) + {}^{E'}\!/_{E} + c_{\rm s}^2 k^2\right.}\,, \tag{6.1.3}$$

where we have used Eq. (4.3.5) to replace derivatives of Ψ with the observable Γ. So given observations of Γ and E, $\hat{Y}\left[c_{\rm s}^2, \Omega_{\rm m0}\right]$ is a functional on that data depending on the parameters $\Omega_{\rm m0}$ and $c_{\rm s}^2$ which outputs a function of scale and time.

However, we should stress that we can *always* find *some* $\hat{Y}$ given *any* data and given *any* choice of parameters. We have therefore thus far only obtained a *model* for Y in the spirit of that provided by (4.3.4). It is a little complicated, in that it depends not only on parameters equivalent to the h_i's, but also on observable data. If the observable Γ shows no scale dependence, in principle we have a very simple model for Y, not dissimilar to the quasi-static one. If on the other hand, the observations do show scale dependence, $\hat{Y}$ could be a very complicated function of scale.

We must now test whether this model for Y is consistent with the observations using the consistency relation (5.2.6). This means that k-*essence* can only be a good description of the dark energy if there is no anisotropic stress observed and also

$$\frac{\hat{Y}'}{\hat{Y}} + \frac{2\Omega_{\rm m0}\hat{Y}}{P_2} = 1 + \Gamma\,,$$

at every redshift and every scale. This consistency relation must be valid given just one global parameter $\Omega_{\rm m0}$ and at each redshift the sound speed $c_{\rm s}^2$ and its derivative. Given

measurements at four scales at any one redshift, it is in principle enough to exclude such a model for Y and therefore k-*essence* as the mechanism for dark energy, assuming the existence of a perfect data set, as we already declared.[2] Note that our approach is independent of the initial conditions.

If given the assumption of k-*essence*, the consistency relation is satisfied at all redshifts, then the above measurements can be used to determine the value of the sound speed at each redshift observed. This allows a non-parametric determination of this physical property that in general is an arbitrary function of time.

It is worth mentioning the limit $c_{\rm s}^2 = 0$ [56, 57], which is not quasi-static on any scale. In such a case, the dust and dark energy perturbations become indistinguishable and the entropy perturbation source in Eq. (6.1.2) disappears, yielding

$$\Psi'' + \left(4 + \frac{E'}{E} + 3\tilde{c}_{\rm a}^2\right)\Psi' + \left(3 + 2\frac{E'}{E} + 3\tilde{c}_{\rm a}^2\right)\Psi = 0\,. \tag{6.1.4}$$

where we have redefined the adiabatic sound speed to be that corresponding to the total EMT, $\tilde{c}_{\rm a}^2 \equiv \dot{p}_X/(\dot{\rho}_X + \dot{\rho}_{\rm m})$, i.e. it is now a function purely of the background geometry. In this limit, there is no dependence on the unobservable $\delta_{\rm m}$ and all scale dependence disappears. A measurement of Y is not possible in a fundamental sense, since there is no difference in the properties of the DE and the DM perturbations. The dark degeneracy is complete. The physics of the linear perturbations is effectively that of a single generalized dust collapsing on a background with some equation of state [57]. However, for such a model to be a valid description of the observations, the data must satisfy the constraint

$$\Gamma' + \left(\Gamma + 3 + 2\frac{E'}{E} + 3\tilde{c}_{\rm a}^2\right)(\Gamma + 1) + \frac{E'}{E} = 0$$

at every redshift and every scale with no free parameters. This constraint reduces to exactly that of ΛCDM when the equation of state for the dark energy becomes -1.

Models with kinetic gravity braiding (KGB) [58, 59] are the most general class of scalar-tensor theories with a single scalar which do not have a direct coupling to gravity and therefore do not have anisotropic stress despite being imperfect fluids [60]. The KGB equivalent of Eq. (6.1.2) would feature more scales, however the prescription for constraining this class of

[2] In fact, this would exclude any single perfect fluid as dark energy, since k-*essence* is equivalent to perfect-fluid hydrodynamics. Multiple perfect fluids or fluids with internal degrees of freedom have in general more complicated pressure perturbations, which would naively appear as more complicated scale dependence (e.g. [55]).

models would not differ from the k-*essence* example presented here.

6.2 Quasi-static Dark Energy

As we have discussed in Ref. [29], perturbations in scalar-tensor dark energy models frequently can be approximated to evolve in the quasi-static approximation, where the dark energy follows the dark matter perturbations and the time derivatives are negligible (see also Ref. [46]). For the Horndeski Lagrangian [48, 49], which is the most general scalar-tensor theory involving no more than second derivatives, this limit was presented in Ref. [61] (we derive it in detail taking a slightly different path in appendix 8.2). This derivation assumes that the only scales relevant to the problem are the Jeans length (determined by the sound speed) and the Compton wavelength, determined by the effective mass of the scalar perturbations. Dispersion relations are in principle more complicated in these models, but apart from the mass, the sound speed does provide the smallest scale by the virtue of being defined in the $k \to \infty$ limit. Under the quasi-static assumption, or that the speed of sound is close to that of light and the scales larger than the Jeans length lie outside of the scales probed by the observations, the effective Newton's constant and the slip parameter (4.3.1) in these general scalar-tensor models take the form

$$Y = h_1 \left(\frac{1 + k^2 h_5}{1 + k^2 h_3} \right) , \quad \eta = h_2 \left(\frac{1 + k^2 h_4}{1 + k^2 h_5} \right) , \tag{6.2.1}$$

where the functions h_i are purely functions of redshift determined by the Lagrangian describing the dark energy model (the explicit form of h_{1-5} is presented in appendix 8.1.1).

The quasi-static limit is really the requirement that the dark energy perturbations follow the dark matter ones in a very constrained way. Dark matter evolves on the geodesics of the combined gravitational potential while the dark energy perturbation must follow the very precise prescription defined by Eqs (6.2.1), without any dynamics of its own.

One can use Eq. (5.1.4) to test the consistency of the observed Universe with the slip parameter η given by the form (6.2.1). As we have described in Ref. [29], given measurements of the observable (5.1.4) at more than three different scales per redshift, we can test whether the data are consistent with a description for η of the form (6.2.1). If not, then the anisotropic stress cannot be described as a manifestation of a scalar-tensor theory in the quasi-static limit.

Since dark matter is supposed to move in a known way on geodesics of the metric and we can map this metric out, the consistency of the form of Y given in the quasi-static limit can be tested, despite the non-observability described in section 4.2. Inserting the form (6.2.1) into the consistency relation (5.2.6) allows one to ask, *redshift by redshift*, whether

the quasi-static form for Y is consistent with the observational data, i.e. whether the simple scale dependence for Y driven by the coefficients h_i is sufficient to explain the observations. As a result of taking the time derivative in (5.2.6), the number of free parameters increases to seven (including $\Omega_{\rm m0}$), thus a larger number of measurements at each redshift is required to overconstrain the system, but it is in principle not any more difficult than for the anisotropic stress.

The main takeaway from this discussion is that if the quasi-static limit can be assumed, the dark energy configuration can be tested by looking for a particular scale dependence of observables redshift bin by redshift bin, rather than as a single integrated fit to the observations with a particular parametrization chosen for the functions h_i.

6.2.1 Scale-dependent test for quasi-static dark energy

With the same spirit of the consistency check developed in section 6.1 we have worked out a consistency relation that depends only on observable quantities. In fact, if we define the following function of the observables R, L and E

$$g(z,k) \equiv \frac{(REa^2)'}{LEa^2}$$

that has the same type of scale-dependence as Eq.(6.2.1), it will satisfy the following consistency test

$$2g^{(1)}g^{(3)} - 3(g^{(2)})^2 = 0\,, \tag{6.2.2}$$

where $g^{(n)}$ is the n-th derivative of g with respect to k^2. If this condition fails at any one redshift, dark energy is not described by the HL in the linear quasi-static limit. Needless to say, a cosmological constant satisfies the consistency relation.

6.3 The Full Horndeski

The structure of the energy-momentum tensor for the general class of Horndeski theories is much more complex than for a model such as k-*essence*. In particular, the Lagrangian features a non-minimal coupling to gravity. This means that the energy-momentum tensors for any such models will feature, in general, anisotropic stress related to the perturbations of the scalar. One can clearly verify this in the anisotropic constraint (that corresponds to the traceless part of the EMT) for this theory

$$\delta T^i_j - {}^1\!/_3\delta^i_j\delta T^k_k \equiv B_6\Phi + B_7\delta\phi + B_8\Psi = 0,$$

Horndeski models in the presence of dark matter have EMTs which have the following dependence on the perturbed fields when linear perturbations are considered [3]:

$$\begin{aligned} \delta T^0_0 &\supset \dot{\delta\phi}, \delta\phi\,, \delta_{\rm m}\,, \\ \delta T^0_i &\supset \dot{\delta\phi}, \delta\phi\,, \theta_{\rm m}\,, \\ \delta T^i_j - {}^1\!/_3 \delta^i_j \delta T^k_k &\supset \sigma\delta\phi\,, \\ \delta T^i_i &\supset \ddot{\delta\phi}, \dot{\delta\phi}, \delta\phi\,, \end{aligned} \tag{6.3.1}$$

in addition to dependence of all the components on the gravitational potentials Φ and Ψ and their time derivatives. Here σ is fully determined as a function of the Horndeski free functions[4]. As compared to k-*essence*, we have the already mentioned anisotropic stress, which is always proportional to $\delta\phi$. The perturbation $\dot{\delta\phi}$ is present in the $(0i)$ components of the energy-momentum tensor, while the pressure perturbation depends on $\ddot{\delta\phi}$. In addition to the above, we have the equation of motion for the scalar field, which is an equation for $\ddot{\delta\phi}$ in terms of all the other variables.

We can clearly see that the only way to suppress the anisotropic stress is to either make the coupling σ very weak, i.e. effectively make the Horndeski terms non-minimally coupled to gravity irrelevant for the dynamics of dark energy, or to suppress the scalar perturbations, which is only possible if the scalar is very massive and not evolving, i.e. it just contributes vacuum energy [62].

Using the equation of motion for the scalar, we can eliminate $\ddot{\delta\phi}$ from the pressure equations. Then, using the Hamiltonian, momentum and anisotropy constraints [corresponding to the (00), $(0i)$ and (ij) Einstein equations, respectively], we can eliminate three further variables: the scalar perturbations $\delta\phi$, $\dot{\delta\phi}$ and the dark-matter density $\delta_{\rm m}$. This is one extra variable as compared to models without anisotropic stress, where the anisotropy constraint equates the two potentials but is not dependent on the configuration of the dark energy degree of freedom. The remaining form for the (ii) Einstein equation is very simple,

$$\begin{aligned} &\sigma\Big[\Phi'' + \alpha_1\Phi' + \alpha_2\Psi' + \left(\alpha_3 + \alpha_4 k^2\right)\Phi\Big] + \\ &\quad + \left(\alpha_5 + \alpha_6 k^2\right)(\Phi + \Psi) = \sigma\alpha_7\Omega_{\rm m} k^{-2}\theta_{\rm m}\,. \end{aligned} \tag{6.3.2}$$

where the parameters α_i are functions of time alone and are fully determined by the Horndeski Lagrangian. Their exact form will not be useful here.

[3] See appendix 8.1 for the full equations of motion and explicit form of the coefficients in terms of the general Lagrangian functions.

[4] It is equivalent to the parameter B_7 in Ref. [61]. It is only non-zero when there is a direct coupling of the scalar to gravity in the action.

We have kept the dependence on σ explicit to show that in the limit of vanishing anisotropic stress, $\sigma \to 0$, Eq. (6.3.2) is not an alternative dynamical equation for the evolution of the potentials Φ. To obtain the evolution equation, one would have to eliminate Ψ for Φ and would obtain a very complicated equation with many scales embedded in its coefficients. One may worry that Eq. (6.3.2) provides a different version of this evolution equation than that obtained for theories with no anisotropic stress. This is not the case: switching off the anisotropic stress reduces Eq. (6.3.2) to an equation which enforces $\Phi = -\Psi$, thus providing no additional information.

Eq. (6.3.2) is *exact* at all scales where linear perturbation theory is valid. In Eq. (6.3.2), all the variables are model-independent observables. Using the extra information from the anisotropic stress constraint, we have eliminated $\delta_{\rm m}$, which is not observable, and thus we can obtain a consistency relation between pure observables required by all Horndeski models with anisotropic stress,

$$\begin{aligned} &\eta\Gamma' + \eta'' + \Gamma\left(\eta\Gamma + 2\eta' + \tilde{\alpha}_1\eta + \tilde{\alpha}_2\right) + \\ &\quad + \tilde{\alpha}_1\eta' + \tilde{\alpha}_3\eta + \tilde{\alpha}_5 + k^2\left(\tilde{\alpha}_4\eta + \tilde{\alpha}_6\right) = \tilde{\alpha}_7\varpi\,. \end{aligned} \tag{6.3.3}$$

where we have redefined the α_i to absorb factors of σ, E or $\Omega_{\rm m}$, or to combine coefficients into single variables.

The relation (6.3.3) [and (6.4.2)] is valid at all linear scales, without the need to involve the quasi-static limit or choose initial conditions. If cosmological data signalizes a detection of non-vanishing anisotropic stress at even just one scale and redshift, we can require that the data satisfy (6.3.3). At any given redshift, the α_i coefficients are just numbers, independent of scale. The observables, Γ, η and ϖ are in principle complicated functions of scale and Eq. (6.3.3) is a non-linear scale-dependent function on these data. Performing observations for at least seven values of k one can form an overconstrained system and rule out the Horndeski model, or confirm it while measuring its parameters α_{1-7}, redshift by redshift without prior parametrization.

6.4 $f(R)$ theory

A nice simple example of the relation (6.3.2) can be obtained in the case of the $f(R)$ class of dark energy models, which are a subclass of the Horndeski Lagrangian and therefore feature much less freedom [63]. Following the algorithm described above, one obtains as the exact

linear result

$$\Phi'' - \Psi' + \left(4 + \frac{E'}{E}\right)\Phi' + \frac{1}{3}\left(m_{\rm C}^2 + 2k^2\right)\Phi + \\ + \frac{1}{3}\left(m_{\rm C}^2 - 6\left(2 + \frac{E'}{E}\right) + k^2\right)\Psi = 0\,, \tag{6.4.1}$$

where $m_{\rm C}^2 \equiv f_{,R}/2H^2 f_{,RR}$ is the Compton mass of the scalar degree of freedom in the units of Hubble. We must have $m_{\rm C}^2 \gg 1$ in order to satisfy Solar-System constraints [64]. At small enough scales, $k \gg m_{\rm C}$, we can recover the standard quasi-static result in $f(R)$ that $2\Phi + \Psi = 0$. Again, we can express the above as a null test on observables that needs to be satisfied at all scales where linear theory is valid

$$\eta\Gamma' + \eta'' + \Gamma\left(\eta\Gamma + 2\eta' + 5 + \frac{E'}{E}\right) + \left(4 + \frac{E'}{E}\right)\eta' + \\ + \frac{m_{\rm C}^2}{3}(\eta - 1) + 6\left(2 + \frac{E'}{E}\right) + \frac{k^2}{3}(2\eta - 1) = 0\,. \tag{6.4.2}$$

This relation has only one free parameter, $m_{\rm C}^2$, which can be freely adjusted at each redshift to fit the data. If this is not enough to satisfy the above test, then $f(R)$ is not a general enough theory to account for the observations.

Part II

The Dark Degeneracy

Gravity can only probe the total energy momentum tensor. Dark matter and dark energy are only detected through their gravitational effect. Because they are "dark" we can only see their effect in the dynamics of galaxies that move on potentials sourced by them, and we cannot know how each component contributes separately to the potentials. Thus, a split of the energy momentum tensor into two components with different properties, e.g. equations of state and sound speed, is completely arbitrary. This is acknowledged as the dark degeneracy.

On the background level, the degeneracy means we don't know the separate values of the energy densities Ω_m and Ω_x. One can see how this manifests in the equation of state of the combined dark fluid $w(z)$, given by

$$w(z) = \frac{H(z)^2 - \frac{2}{3}H(z)H'(z)(1+z)}{H_0^2\Omega_m(1+z)^3 - H(z)^2}. \tag{6.4.3}$$

As we have elucidated in section 4.1, background observables can in principle probe the background evolution through the Hubble parameter $H(z)$. Notice in Eq.(6.4.3), how one can always find a value of Ω_m that reproduces the expansion history for *any* choice of $w(z)$. As remarked by Kunz in [36], numerous analysis try to constrain $w(z)$ with background probes while assuming a certain parametrization. However, this ends up imposing strong priors on the type of dark energy.

One could ask whether this feature is restricted to the background level, and if linear perturbations could provide more information and break the degeneracy. However, the dark degeneracy remains at the perturbative level, e.g. it limits our knowledge about the effective gravitational coupling Y. This is clear from its definition, $Y \equiv -2k^2\Psi/3\Omega_{\rm m}\delta_{\rm m}$, as well as from the consistency relation for it:

$$\frac{Y'}{Y} + \Omega_{\rm m0}\varpi Y = 1 + \Gamma\,, \tag{6.4.4}$$

In order to solve the differential equation for Y, we need to provide an initial condition. By using its definition, we find the equivalent equation

$$\frac{\delta_m'(a)}{\delta_m(a)} + \frac{\Psi'(a)}{\Psi(a)} + \frac{k^2A(a)\Psi(a)}{\delta_m(a)} + B(a) = 0, \tag{6.4.5}$$

where $A(a)$ and $B(a)$ are observables, whose particular forms are not relevant. As all terms in this equation are observable quantities, except for $\delta_m(a)$, it is evident that the initial condition to provide is the unknown initial value of the density perturbation $\delta_{m\,i}$.

A similar analysis was done by Kunz and Sapone in [33]. The authors have argued that the dark matter growth factor $G \equiv \delta_m/\delta_{m0}$ is not uniquely determined by the expansion

history. Additionally, it responds to a choice of the dark energy sound speed [5]. If the sound speed is small, the clustering of dark energy increases and so the sourcing of the gravitational potentials where dark matter falls. Therefore, the smaller the dark energy sound speed, the more dark matter clusters.

On the next chapter we will explore this degeneracy by making two splits in the energy momentum tensor. We distinguish dark matter and dark energy by assuming a fiducial ΛCDM model. Furthermore, we split dark matter into a cold and a hot component by introducing a conversion process [30].

[5] They have assumed the observability of G for this analysis, although that's not the case unless the bias is known.

Chapter 7

A dark matter model

Introduction

In Part I of this thesis we developed a testing strategy trying to be as agnostic as possible on the level of assumptions, specially by refraining from assuming a dark energy model. We will now follow a completely opposite route, more closely to the standard approach on data analysis, and consider a model that is a small departure of the ΛCDM. In this sense, the two parts of the thesis are completely independent and make two very distinct type of analysis. This enriches our perspective on the two approaches, allowing us to compare them, and to put the dark degeneracy in evidence in two different ways.

We haven't yet directly detected a dark matter particle, if there is any. Furthermore, specially regarding the small scales, many controversies remain unsettled, e.g. the core-cusp [65, 66] and the missing satellites problem [67, 68]. Generally, simulations of structures produce dark matter halos with a very steep profile, not matching observations, and the number of substructures around galaxies predicted by simulations is superior than the observed one. Efforts have been made in an attempt to improve both simulations and observations, but a general disagreement remains between approaches and results from different groups.

Naturally, many alternative scenarios have been proposed to deal with the small scales issues, where dark matter, or at least a fraction of dark matter, is not cold. The free streaming length of the DM particle limits the size of structures, setting the mass of a warmer candidate around the keV scale in a scenario in which this candidate is dominant. A dark matter particle with this mass scale could be a sterile neutrino [69]. Some recent proposals of warm and warm+cold dark matter cosmologies have shown that a standard warm dark matter (WDM) cosmology does not solve the core-cusp problem [70]. Furthermore, a warm dark matter scenario naturally leads to a smaller number of satellites [71]. However, other scenarios are not excluded, e.g. the decay of cold thermal relics [72, 73]. On the other hand,

the effect of baryons potentially plays a significant role in the galaxy dynamics [74] and still presents a challenge for simulations. Accounting for the baryonic effects can lower the number of subhalos as pointed out in ref. ([75, 76]), however it is not yet certain whether a CDM+baryonic processes can reconcile simulations and observations of Milky Way satellites. More recently, there are claims [77] that gas outflows from stellar activity can significantly attenuate the steepness of the core. A proposal [78] of long range interactions between cold dark matter particles also would be able to dynamically settle the issue. Still in the spirit of mixed scenarios, it is interesting to see how cosmology can constrain limits on hot dark matter particles, like neutrinos or axions [79].

7.1 Conversion model

We will not assess the particle nature of dark matter. As we have argued, a cosmological scenario allows for a split in the energy momentum tensor of dark matter. From structure formation, we know that such split should not produce a large amount of a relativistic component, specially in the matter dominated epoch. We consider a general conversion process of dark matter into dark radiation and analyze how this is constrained by cosmology. Naturally, the particles are not collisionless, but we don't make any restrictions about the interactions that could lead to conversion. Our work is inspired on processes in the baryonic sector that convert non-relativistic into relativistic matter. Known astrophysical phenomena can cause such conversions, like accretion disks around black holes and supernovae events, the latter being the most interesting for us due to the large amount of energy released as relativistic neutrinos.

When the gravitational pressure of a star exceeds the degeneracy pressure of electrons, the star explodes (or collapses) releasing radiation and neutrinos. The energy budget of the relativistic species is mostly carried by the neutrinos. Typically, this energy corresponds to 99% of the binding energy of the remnant neutron star. We consider the net effect of this phenomena as a starting point to suppose that a similar process can occur in the dark sector, and perform a phenomenological study about the limits in a late time and environmental conversion of cold dark matter into dark radiation. There are many different models with such a transition, e.g. in ref. ([80, 81]), where dark matter decays at earlier times and in ref. ([82, 83]) where a coupling neutrino-quintessence accelerates neutrinos to relativistic velocities in scales of order of Mpc in the recent Universe.

7.1.1 Supernova production rate

Most models of supernova neutrino flux are built from direct observation of core collapse supernovae. However this method only provides a good parametrization for small redshifts, and since we are interested in the effects of such production rate in all cosmological history, we will use a model where the time-dependent supernova rate $R_{SN}(z)$ is proportional to the star formation rate $R_{SF}(z)$ [84, 85, 86, 87, 88]

$$R_{SN}(z) = \frac{\int_{8M_\odot}^{50M_\odot} \phi(m)dm}{\int_{0.1\odot}^{125M_\odot} m\phi(m)dm} R_{SF}(z) \ , \tag{7.1.1}$$

and the star formation rate is parametrized as

$$R_{SF}(z) = h\, 0.3 \frac{e^{3.4z}}{e^{3.8z}+45} [M_\odot.\mathrm{yr}^{-1}\mathrm{Mpc}^{-3}] \ . \tag{7.1.2}$$

We normalize the rate by considering the number of stars that would most likely undergo a supernova event with a correspondent emission of neutrinos, from $8M_\odot$ to $50M\odot$. This can be obtained through the integration of the initial mass function

$$\phi(m) \propto \begin{cases} m^{-2.35} & ; \quad 1M_\odot < m \\ m^{-2.33-1.82\log m} & ; \quad 0.1M_\odot < m < 1M_\odot \end{cases} \ . \tag{7.1.3}$$

where we used the combined Salpeter [89] and Gould [90] initial mass functions in the appropriate mass intervals [91].

As it is well known, relativistic neutrinos are the main energetic output from a supernova explosion, where $\sim$ 99% of the progenitor gravitational binding energy is transferred to neutrinos. As a consequence, a diffuse supernova neutrino flux is present in our Universe. The energy density carried by these neutrinos can be calculated from the evolution equations:

$$\dot{\rho}_b = -3H\rho_b - \bar{E}_\nu R_{SN} \ , \tag{7.1.4}$$

$$\dot{\rho}_\nu = -4H\rho_\nu + \bar{E}_\nu R_{SN} \ , \tag{7.1.5}$$

where $H = \dot{a}/a$ is the Hubble parameter and $\bar{E}_\nu \sim 3\times 10^{53}$ erg is the total energy carried by the neutrino flux in a supernova explosion. The solutions to these equations are given by:

$$\rho_b = \frac{1}{a^3}\left[\rho_0 - \int^a a^3 \bar{E}_\nu R_{SN} dt\right] \ , \tag{7.1.6}$$

$$\rho_\nu = \frac{1}{a^4}\int^a a^4 \bar{E}_\nu R_{SN} dt \ . \tag{7.1.7}$$

In figure 7.1.1 we can see the profile of energy density carried by relativistic neutrinos produced by SN explosion as a function of redshift. In the same plot we show the energy density carried by relativistic species created in dark-matter decay, where the parameters were chosen to produce the same amount of energy density of relativistic species. It is possible to see from figure 7.1.1 that two very different mechanisms can produce similar patterns of relativistic species production.

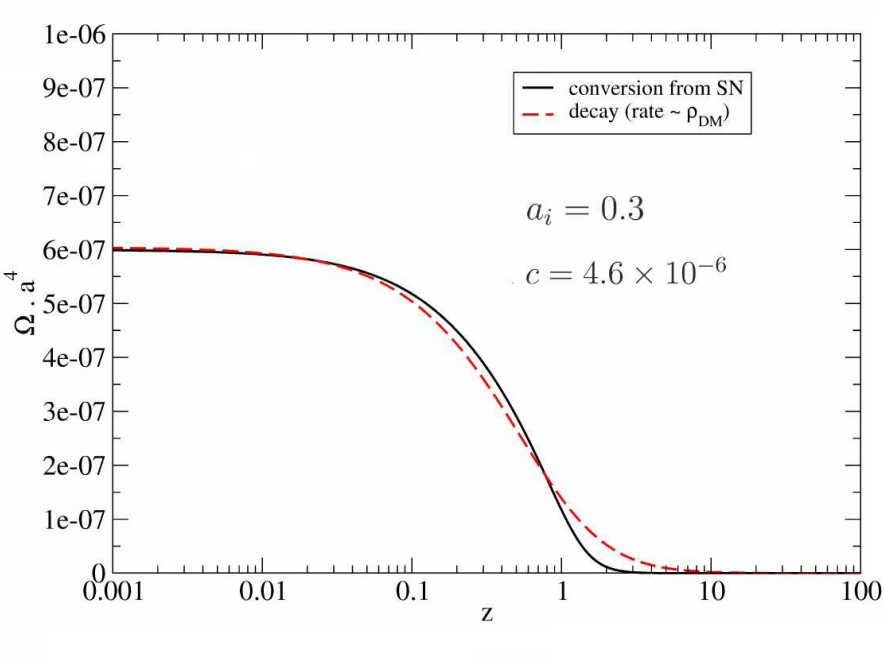

Figure 7.1.1: The supernova produced neutrino density fraction, $\Omega = \rho_h/\rho_{cr}$, as a function of z.

We propose a scenario where cold dark matter is converted into dark radiation (with a not initially populated distribution) by a generic mechanism that is not necessarily the decay of the original cold dark matter particle content, but resembles the production mechanism of supernova neutrino. We chose the following *ansatz* for the cold dark matter density evolution

$$\rho_c a^3 = \begin{cases} \rho_0 & ; a < a_i \\ \rho_0 e^{-\kappa(a-a_i)} & ; a > a_i \end{cases} , \tag{7.1.8}$$

where a_i defines a starting time for the conversion and κ, the rate at which this conversion occurs. The evolution equations can then be easily integrated, and we obtain for the relativistic dark matter density

$$\rho_h a^4 = \begin{cases} 0 & ; a < a_i \\ \rho_{c_0}\left(a_i + \frac{1}{\kappa}\right) \times \left[1 - e^{-\kappa(a-a_i)}\right] & ; a > a_i \end{cases} . \tag{7.1.9}$$

With this parametrization, the conversion profile on SN neutrinos can be fairly reproduced by the the choice $a_i = 0.3$ and $\kappa = 4.6 \times 10^{-6}$. This indicates that our parametrization presents a good versatility and a close connection to known astrophysical processes, where a conversion from non-relativistic to relativistic matter occurs.

When constraining our parameters, it is more convenient to work with variables that gives us directly the amount of dark matter in a relativistic form today. This can be calculated explicitly by:

$$F = \left.\frac{\rho_h}{\rho_c + \rho_h}\right|_{a=1} \quad . \tag{7.1.10}$$

The correspondence between the parameter κ and F, for a given value of a_i, is unique, and can be obtained numerically from the relations above. We present this correspondence in figure 7.1.1.

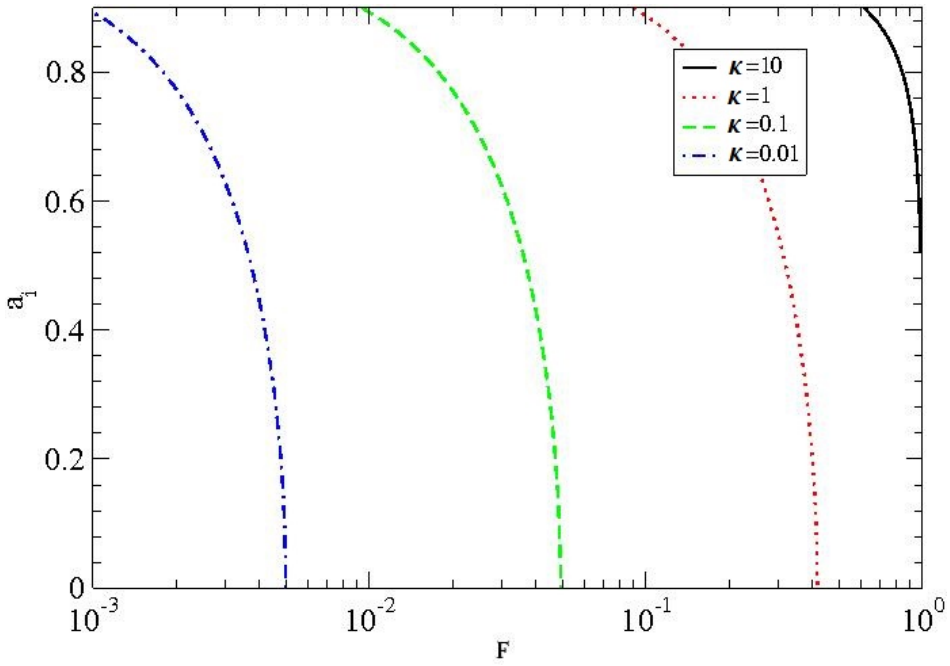

Figure 7.1.2: Values of parameter κ from F and a_i.

7.2 Boltzmann equations

Perturbations over the homogeneous background of the cosmic ingredients can be evolved as a series of coupled Boltzmann equations of perfect fluids, where each component is fully described as a hierarchized set of equations, truncated according to its thermal condition and coupled according to the physics considered. For a complete description of all the components, see the ref. ([92]). In this thesis, it is going to be detailed only the set of equations of cold

dark matter and dark radiation with the environmental conversion as a coupling.

We suppose that cold dark matter particles have a mass m_c that undergo an environmental conversion at a rate dg_c/da to dark radiation with an empty distribution populated at a rate dg_h/da. The Boltzmann equation for the cold dark matter is

$$\frac{df_c}{dt} = C\left[f_c\right]. \tag{7.2.1}$$

In this scenario with dynamical dark matter, the total distribution function depends on the momentum and the scale factor, we also consider that the dependencies are detachable

$$C[f_c(p,a)] = -\dot{a} f_c(p) \frac{dg_c(a)}{da}, \tag{7.2.2}$$

where the function $g_c(a)$ represents an effective and already normalized conversion process. We consider that the phase space of the daughter particle is completely available. Integrating the distribution function, the final equations of density are

$$\dot{\rho}_c + 3\frac{\dot{a}}{a}\rho_c = -a\dot{a}\frac{dg_c(a)}{da}\rho_c, \tag{7.2.3}$$

and density perturbations are

$$\dot{\delta}_c + ikv_c + 3\dot{\Phi} = -a\dot{a}\frac{dg_c(a)}{da}\delta_c. \tag{7.2.4}$$

For non-relativistic particles is enough to extend the hierarchical description to the velocity term

$$\dot{v_c} + \frac{\dot{a}}{a}v_c + ik\Psi = -a\dot{a}\frac{dg_c(a)}{da}v_c, \tag{7.2.5}$$

any higher order effects, such as pressure or stress are negligible and even undesirable, since they are not observed in the clustering of dark matter. In a similar way, we detail the equations of density and density perturbations of the dark radiation, which is identical to the massless neutrino equations except for a non-null collision term

$$\frac{df_h}{d\tau} = C\left[f_h\right]. \tag{7.2.6}$$

The distribution of relativistic particles in thermodynamical equilibrium is completely described by the temperature. We assume that this is the case and include the perturbations directly in the distribution function

$$f_h(x^i, p_j, \tau) = f_{h0}(p,\tau) \times [1 + \Psi(x^i, p, n_j, \tau)]. \tag{7.2.7}$$

The collision term populates the dark radiation from the cold dark matter distribution

$$C[f_h(p,a)] = -\dot{a} f_c(p) \frac{dg_h(a)}{da} = \dot{a} f_c(p) \frac{dg_c(a)}{da}. \tag{7.2.8}$$

The density of the relativistic particles will be given by

$$\dot{\rho}_h + 4\frac{\dot{a}}{a}\rho_h = a\dot{a}\frac{dg_c(a)}{da}\rho_c. \tag{7.2.9}$$

By integrating again the perturbed distribution function, but this time taking the expansion in Legendre polynomials, a hierarchical system of equations describing the perturbations in the dark radiation temperature is obtained, where the monopole term is

$$\dot{\delta}_h = -\left(\frac{4}{3}\theta_h - \dot{a}\frac{dg_c(a)}{da}\delta_c - 4\dot{\phi}\right), \tag{7.2.10}$$

and the dipole

$$\dot{\theta}_h = \left[k^2\left(\frac{1}{4}\delta_h - \sigma_h\right) + k^2\psi\right], \tag{7.2.11}$$

which can be used to obtain the whole set of equations by the recurrence formula

$$\dot{\mathscr{N}_l} = \frac{k}{2l+1}\left[l\mathscr{N}_{l-1} - (l+1)\mathscr{N}_{l+1}\right], l \geq 2, \tag{7.2.12}$$

until some order of truncation l_{max}, where

$$\mathscr{N}_{l_{max}+1} \approx \frac{(2l_{max}+1)}{k\tau}\mathscr{N}_{l_{max}} - \mathscr{N}_{l_{max}-1}. \tag{7.2.13}$$

For the desired density conversion given by equation 9, the *ad-hoc* conversion rate must be

$$\frac{dg_c(a)}{da} = \frac{\kappa}{a}, \tag{7.2.14}$$

which replaced in eqs. (7.2.3) and (7.2.9), gives

$$\rho_c = \frac{\rho_{c_0}}{a^3} \times e^{-\kappa(a-a_i)}, \tag{7.2.15}$$

$$\rho_h = \frac{\rho_{c_0}(a_i + \kappa^{-1})}{a^4} \times \left[1 - e^{-\kappa(a-a_i)}\right], \tag{7.2.16}$$

as planned beforehand in eqs. (7.1.8) and (7.1.9). Given that the conversion is supposed to be an environmental effect related to the galaxy halo, we include a scale dependence of the

form

$$\frac{dg_c(a,k)}{da} \rightarrow h(k,k_g) \times \frac{dg_c(a)}{da}, \tag{7.2.17}$$

$$\frac{dg_h(a,k)}{da} \rightarrow [1-h(k,k_g)] \times \frac{dg_h(a)}{da}, \tag{7.2.18}$$

where the term included is a smooth step function and k_g is defined as the scale where the conversion reaches half of its maximum effect for each redshift.

7.3 Statistical Analysis

Table 7.1: Parameters of the model and their flat prior. The first six parameters in the first block belong to the so called "vanilla" cosmological model. The middle block contains extended standard parameters that are expected to have degeneracy with the conversion model parameters. The last block contains the parameters added by our model of dark matter conversion.

Type	**Parameter**	**Description**	**Min**	**Max**
Vanilla	$\Omega_b h^2$	Baryon density	0.005	0.1
	$\Omega_c h^2$	Cold dark matter density	0.04	0.18
	θ	Ratio between the sound horizon and the angular diameter distance at decoupling	0.5	10
	τ	Reionization optical depth	0.01	0.8
	n_s	Spectral index of primordial power spectrum at $k = 0.05h\text{Mpc}^{-1}$	0.5	1.5
	$log[10^{10}A_s]$	Amplitude of primordial power spectrum at $k = 0.05h\text{Mpc}^{-1}$	2.7	4.0
Extended	f_ν	Fraction of neutrino density related to the dark matter	0	0.1
	w	Parameter of dark energy constant equation of state	-1.5	0.5
Extra	a_i	Scale factor when the conversion starts	0.1	1.00
	κ	Rate of conversion	0	2

The statistical analysis was made by Markov Chain Monte Carlo (MCMC) using the data from the anisotropies of the Cosmic Microwave Background measured by the WMAP, the matter power spectrum measured by the SDSS and the type Ia supernovae luminosity compiled by the Union-2. Best fits were obtained by conventional χ^2 analysis using Bayes posterior probability description. All priors used were flat distributions over the range tested. We run the CosmoMC [93] package of MCMC to test the theoretical predictions generated by a modified version of CAMB [94], which included the particles described by the Boltzmann equations developed in section 7.2. Besides the standard parameters for cosmology, our model

add the parameters listed in the last block of table 7.1. The priors adopted are the standard for the vanilla parameters, while the prior for the parameter κ goes from vanishing conversion ($\kappa = 0$) to non-physical values ($\kappa = 2$) when all the cold dark matter is quickly converted, for the parameter a_i the prior goes from conversion starting today ($a_i = 1$) to non-physical values ($a_i = 0.1$) when the dark radiation strongly degrades the structure formation. This choice for the extra parameters obeys the rule to stipulate a prior that encompasses a vanishing effect and non-physical results in such a way that the posterior probability has a well defined tail. In our case, this criteria for prior stipulation are especially designed to include galaxy's surveys, which are our target and consequently the most affected observable. The scale conversion k_g was fixed to the scale of typical galactic halo size, $k_g \equiv 0.2$ Mpc^{-1}. The convergence requirement followed the Gelman and Rubin R statistic, which states that the variance of chains means divided by the mean of chains variances must approach one. In this work, we reached a convergence of at least $R - 1 < 0.05$, which could be regarded as a low convergence, but taken into account that the CosmoMC package is adjusted for statistical efficiency when fitting the standard cosmological model, we consider that for a first time fitting, the condition $R - 1 < 0.05$ for an alternative model is acceptable.

Because there is an obvious degeneracy between neutrino density and any other kind of dark radiation, we included the fraction of dark matter in massive neutrinos f_ν among the standard parameters of ΛCDM, distributing the density of neutrinos equally among three states and fixing the number of families to $N_{\rm eff} = 3.04$. It is also expected to exist a correlation between the effects of dark matter conversion and the parameter w of the dark energy equation of state [95]. For this reason this parameter was included in our analysis.

7.4 Results

By fitting the data with theoretical predictions, we calculate chains of the likelihood for all parameter values inside the ranges delimited. The complete dataset fitted was WMAP + SDSS + SNIa and the likelihood functions adopted for each observable were the ones suggested in their respective papers. We present in table 7.2 for each parameter p, the total mean value ($\langle p \rangle$) of its distribution and its confidence level corresponding to the 95% central credible interval to represent the data. In table 7.2, we also present the best fit value ($\hat{p}$) of each parameter and its confidence level corresponding to the 2σ probable region. In this case, all parameters values are kept in the total best fit point. When the limits are not shown means that the limit is compatible with the correspondent limit in its prior range. See ref. ([96]) for different statistical approaches and their relevance in cosmology. In order to compare and qualify the modified model, we also present the mean and best fit points, the

credible regions and confidence levels of the standard cosmological model. We use ΛHCDM as the acronym for the model with dark matter conversion, while keeping ΛCDM for the standard model, both extended with massive neutrinos (m_ν) and an arbitrary value for the dark energy equation of state parameter (w).

When comparing the best fits, the minimal χ^2 for the model with dark matter conversion depreciates the fit for the following amount

$$\Delta\chi^2 = \left(\chi^2_{\Lambda\text{HCDM}} - \chi^2_{\Lambda\text{CDM}}\right)/\Delta d.o.f. = 1.01/2. \tag{7.4.1}$$

For two extra degrees of freedom, this number means that the best fit for ΛHCDM is worse than the ΛCDM best fit, but it is withing 1σ of confidence around the standard model best fit. The best fit point in the likelihood for the two extra parameters that characterize our model are

$$\kappa = 0.6\ , \quad a_i = 0.6\ , \tag{7.4.2}$$

where the large standard deviation prevents better precision. These values for the global best fit correspond to a rate of converted dark radiation over cold dark matter of around 50% in our Universe today.

In figure 7.4.1 we show the matter power spectrum from SDSS, the predictions for ΛCDM and the predictions for our model with dark matter conversion. In figure 7.4.2 we show the correlation between the parameters a_i and κ. The confidence region for the two parameters combined was obtained while fixing the value of standard parameters to their total mean. In this case the set $\{a_i, \kappa\}$ excludes vanishing conversion $\{a_i, \kappa\} \to \{1, 0\}$ at 2σ. However, one should not take this as a preference for conversion. The other parameters are marginalized over in their total mean, which are significantly different from the standard model mean, therefore, the conversion is needed to restore the desirable evolution of the Hubble parameter. This take us back to the discussion on the dark degeneracy. As we have already pointed out, the model parameters are degenerate and the equation of state $w(z)$ can be adjusted in order to reproduce the expansion history $H(z)$ for any value of Ω_m.

In fact, the likelihood posterior distributions of the parameters, a_i and κ, are each separately compatible with vanishing conversion, even at 1σ. The implication for this lack of reducibility is that the conversion cannot be taken as a simple subleading effect. Once it is included, the conversion must be non-vanishing to reach a best fit closer to the one obtained with the standard model.

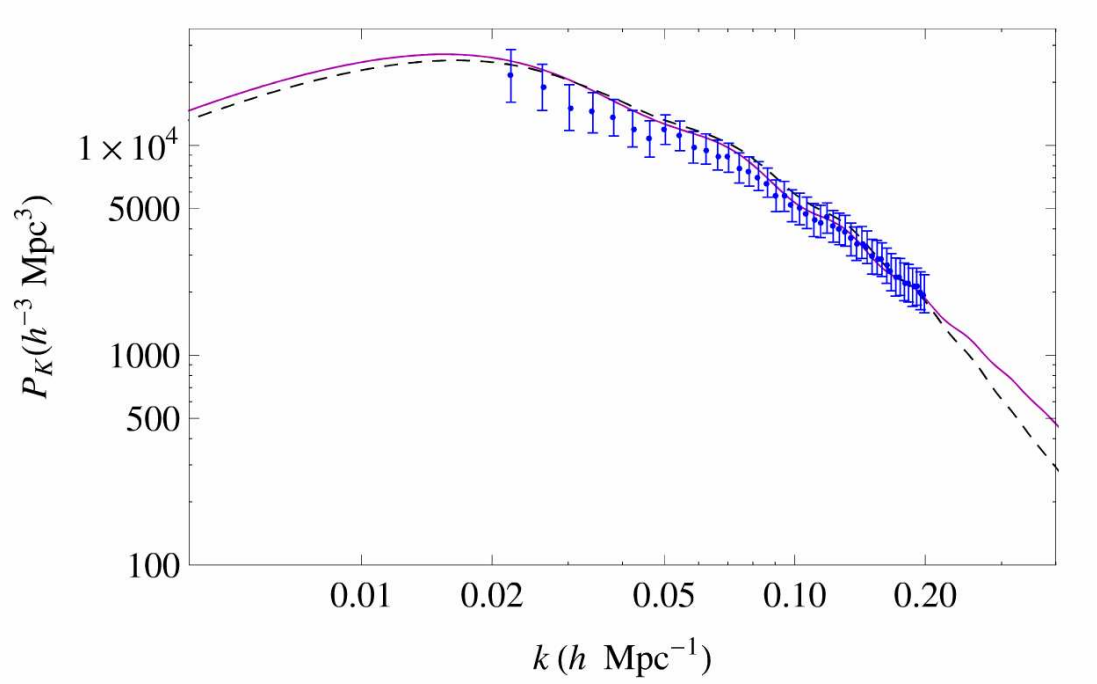

Figure 7.4.1: Matter power spectra for different models containing the best fit for WMAP+SDSS+SNIa. ΛCDM (magenta continuous line) and the model with dark matter conversion (black dashed). SDSS data are shown in blue points, but only diagonal elements of the covariance matrix.

Despite the loss of direct compatibility among the standard parameters when comparing the two models, it is interesting to notice how some of them can be relaxed or tightened, such as the dark energy equation of state parameter, the cold dark matter density or the neutrino masses. Although the parallel between best fits is the main criteria to qualify an alternative model, we show the relaxation of some parameters since it could be useful to explain some isolated effects related to specific parameters detached from the general model.

The conversion of cold dark matter into dark radiation decreases the dark energy equation of state parameter to lower values, to compensate for the creation of matter whose density dilutes with a higher order of the scale factor. This effect is compatible with what is expected when the neutrino masses are increased, which increases the amount of hot dark matter.

The last and most interesting side effect of our conversion model would be the smaller value for the cold dark matter density at late times, specially in the central cores where it is expected to happen the conversion. The decrease in density is desirable given the incompatibility between the cusp galactic centers predicted by n-body simulations and the core profile observed in all surveys [97].

For instance, in the figure 7.4.3 we show the likelihood posterior distribution for all the standard model parameters, primitive and derived ones, with dark matter conversion, and

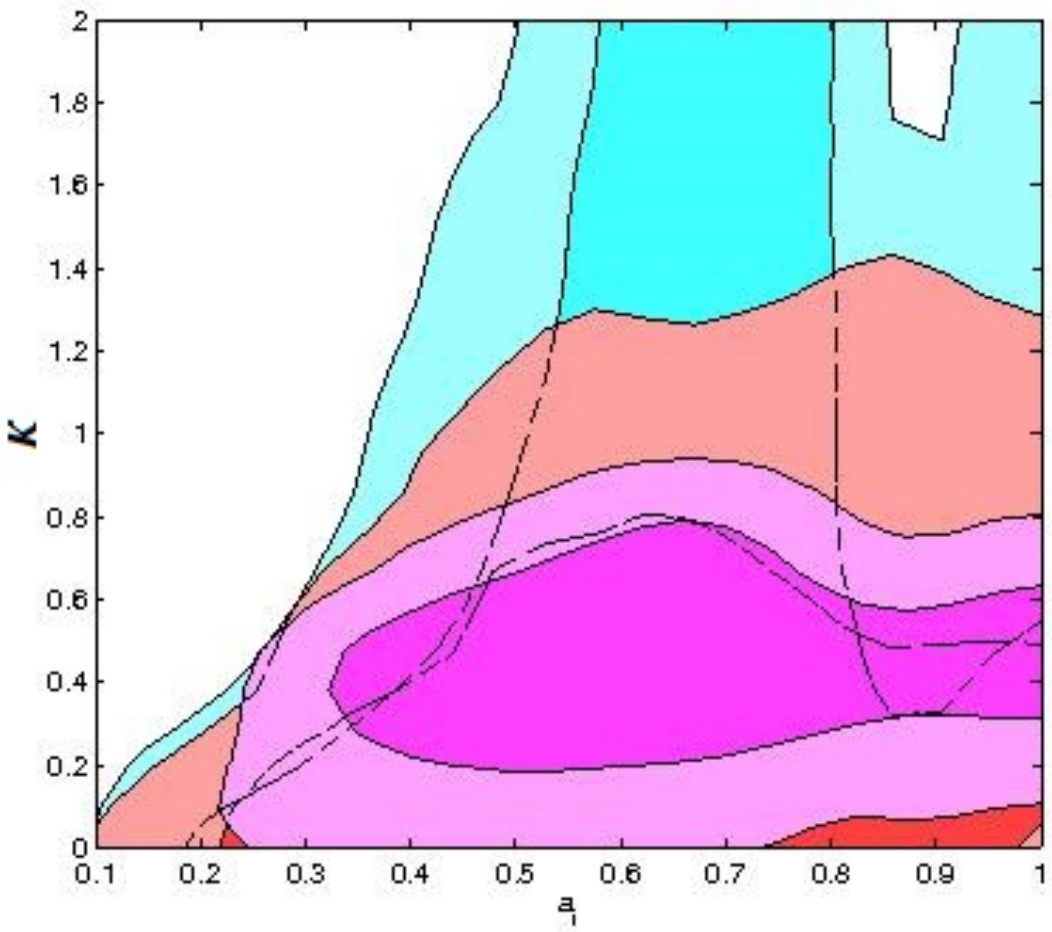

Figure 7.4.2: Correlation of the parameters a_i and κ at 68% CL and 95% CL. All others parameters are marginalized over their total mean values. The confidence regions correspond to the fits obtained with the following data sets: WMAP+SNIa (cyan), WMAP+SDSS (red) and WMAP+SDSS+SNIa (magenta).

the distribution for ΛCDM. It can be seen that the largest deviation on primitive parameters happens for the total amount of dark matter density Ω_c. Given that the conversion decreases the amount of cold dark matter at late times, it is not unexpected that the fitting procedure found a best fit with small density today for cold dark matter while keeping its early time density compatible with the found in ΛCDM scenario. Such concentrated effect in cold dark matter density is not accidental, since the conversion model was built to diminish the dark matter density at small scales without affecting the nice agreement with large scale structures. The deviations from the other primitive parameters with respect to the scenario with no conversion are generally small and with hardly observable effects.

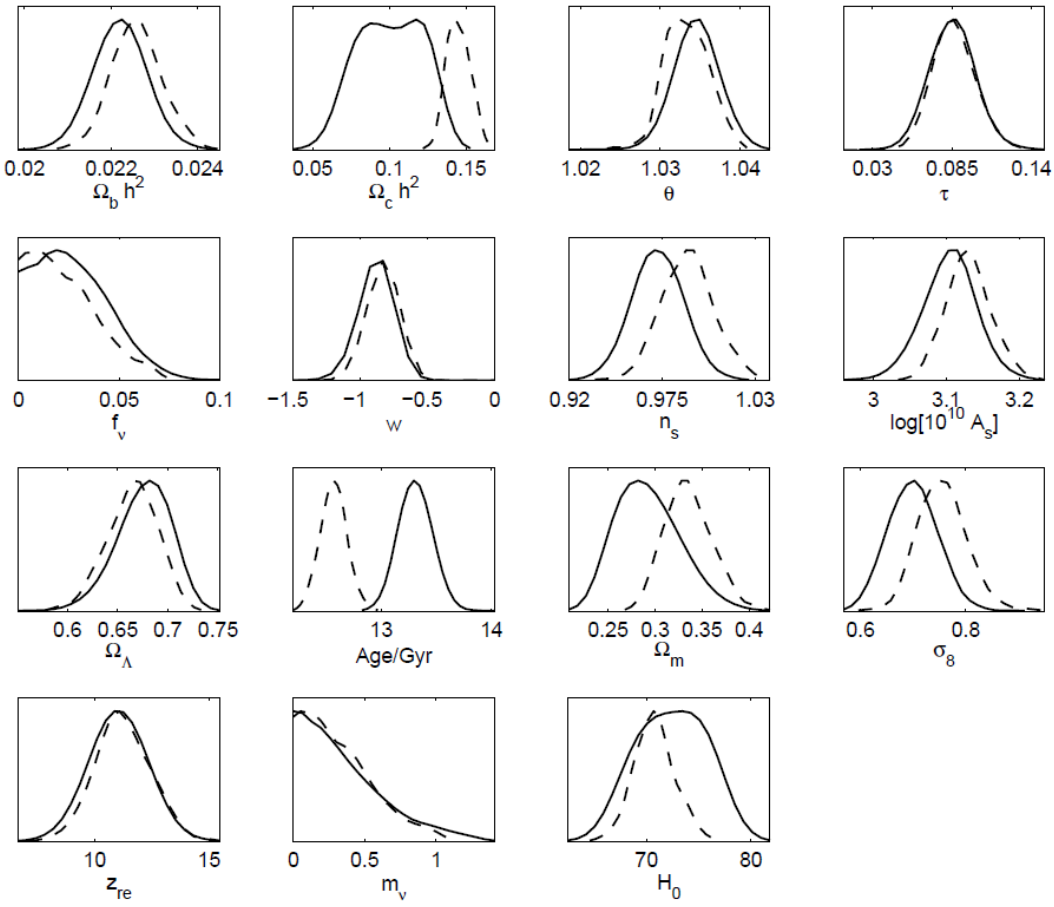

Figure 7.4.3: Posterior normalized distributions for all the standard model parameters for ΛCDM (dashed line) and for the model with dark matter conversion (solid line). All others parameters are marginalized over their total mean values.

Table 7.2: Mean total values $\langle p \rangle$ with their 95% central credible intervals and the best fits $\hat{p}$ with their confidence levels at 2σ, for the model with conversion (ΛHCDM) and for the standard model (ΛCDM). The fits were obtained with WMAP+SDSS+SN data.

Type	**Parameter**	$\langle p \rangle$(95% CCI)		$\hat{p}$ (2σ CL)	
		ΛHCDM	ΛCDM	ΛHCDM	ΛCDM
Vanilla	$\Omega_b h^2$	$0.0222^{0.0234}_{0.0211}$	$0.0226^{0.0238}_{0.0214}$	$0.0223^{0.0245}_{0.0202}$	$0.0226^{0.0246}_{0.0209}$
	$\Omega_c h^2$	$0.10^{0.14}_{0.06}$	$0.145^{0.160}_{0.132}$	$0.07^{0.16}_{0.03}$	$0.142^{0.165}_{0.122}$
	θ	$1.035^{1.040}_{1.030}$	$1.033^{1.039}_{1.028}$	$1.035^{1.053}_{1.024}$	$1.034^{1.042}_{1.024}$
	τ	$0.09^{0.12}_{0.06}$	$0.08^{0.11}_{0.07}$	$0.09^{0.15}_{0.04}$	$0.09^{0.13}_{0.05}$
	n_s	$0.973^{1.002}_{0.943}$	$0.99^{1.02}_{0.96}$	$0.98^{1.02}_{0.92}$	$1.00^{1.04}_{0.94}$
	$log[10^{10} A_s]$	$3.11^{3.18}_{3.03}$	$3.13^{3.19}_{3.07}$	$3.10^{3.24}_{2.98}$	$3.14^{3.23}_{3.04}$
Extended	f_ν	$0.03^{0.06}$	$0.02^{0.06}$	$0.02^{0.10}$	$0.02^{0.07}$
	$-w$	$0.88^{0.74}_{1.06}$	$0.83^{0.71}_{0.98}$	$0.88^{0.63}_{1.31}$	$0.82^{0.62}_{1.13}$
Derived	Ω_Λ	$0.68^{0.72}_{0.62}$	$0.66^{0.71}_{0.61}$	$0.70^{0.76}_{0.54}$	$0.68^{0.73}_{0.58}$
	Age/Gyr	$13.3^{13.6}_{13.0}$	$12.6^{12.8}_{12.3}$	$13.2^{13.8}_{12.8}$	$12.5^{13.0}_{12.2}$
	σ_8	$0.71^{0.80}_{0.63}$	$0.76^{0.85}_{0.68}$	$0.72^{0.89}_{0.58}$	$0.78^{0.92}_{0.62}$
	z_{re}	11^{14}_{8}	11^{14}_{9}	11^{16}_{6}	11^{15}_{7}
	H_0	69^{73}_{65}	71^{75}_{67}	71^{77}_{61}	72^{77}_{65}
	$\sum m_\nu$(eV)	$0.4^{0.8}$	$0.3^{0.8}$	$0.09^{1.4}$	$0.2^{1.1}$
Extra	a_i	$0.6_{0.3}$	N/A	0.6	N/A
	κ	$0.4^{0.8}$	N/A	$0.6^{1.0}$	N/A
Extra derived	$\Omega_h h^2$	$0.06^{0.10}$	N/A	$0.07^{0.13}$	N/A
	F	$0.4^{0.6}$	N/A	$0.5^{0.7}$	N/A

Chapter 8

Discussion

Dark matter is dark. This statement is obvious and yet the discussion of cosmological observations is usually framed as a discussion of the measurements of the dark-matter distribution. This is of course completely natural in the case where there are no dark energy perturbations, i.e. within the framework of ΛCDM cosmology. However, the moment that we relax this assumption, as we must do when investigating dark energy models different from a cosmological constant, this connection between measurements and the dark-matter distribution is no longer simple, and can to all intents and purposes disappear.

We have emphasized that the probes we hope to use to constrain general dark energy models depend on tracers which propagate on geodesics: light for weak lensing and galaxies for RSD. This allows us to map out the metric on our past lightcone (the potentials Φ and Ψ) through which these tracers fall freely. These are the real physical observables of the combination of the cosmological probes. The relation of these potentials to the dark-matter distribution is then a model-dependent statement, which just happens to be an identity for ΛCDM.

Given this limitation, we should stress that the cosmological probes still can provide an enormous amount of information. Since we can reconstruct the potentials, the slip parameter η of the matter/light Jordan-frame metric is a model-independent observable, given overlapping WL and RSD measurements. We do not need to parametrize it and we can answer the question of whether anisotropic stress is at all necessary, directly from observations, without any further modeling. This test has the power to immediately eliminate very large classes of models, whatever its result. If $\eta \neq 1$ at even one redshift and scale, then models without non-minimal coupling to gravity in the baryons' Jordan frame can be thrown away. If $\eta = 1$ everywhere, then such couplings of dark energy to gravity could in principle still be there, but they are so small that they cannot at all influence the dynamics of the Universe and therefore can be neglected. We have summarized the most important dynamical variables

and their observability status in table 5.1.

We have also shown that the evolution rate of the *potentials* can be mapped out. On the other hand, the fact that we cannot observe the dark matter density amplitude means that the effective Newton's constant Y is not an observable in a model-independent setting. Given these model-independent observables, we should refocus the predictions of perturbation theory in dark energy models to their impact on these gravitational potentials rather than on the dark matter, contrary to the dominant approach in the discussion today.

Nonetheless, we have demonstrated in chapter 6 how to construct tests of very general classes of models of dark energy, even away from the frequently employed quasi-static limit. The distinct advantage of this approach is that rather than parametrizing the free functions of a class of models first, then evolving the predictions of these models using modified codes and simultaneously fitting to data, our method is capable of testing/constraining classes of models without any prior parametrization and without any assumptions on the initial conditions. These tests involve performing measurements of the observables at multiple scales, redshift by redshift, with the number of data points required determined purely by the number of free functions of time in the particular class of models. In order to carry out this test it is not necessary to modify codes for each class of models, but just to apply appropriate transformations to the observed data. In other words, our approach calls for exploring the space domain rather than the time domain of dark energy.

We have assumed that there is no velocity bias between dark matter and the galaxies. Thus a measurement of galaxy peculiar velocities $\theta_{\rm gal}$ via RSD is automatically a measurement of the dark-matter peculiar velocity $\theta_{\rm m}$. Statistical origins of the velocity bias notwithstanding [40], there could in principle be a non-vanishing bias between these two velocities. Indeed, this happens in any model in which there is a fifth force acting on dark matter, which does not couple to baryons or light, i.e. models with a violation of the Equivalence Principle such as coupled quintessence [41]. This fifth force is a new source of acceleration for dark-matter particles, causing their peculiar velocities to deviate from that of the galaxies. The effect of this is to introduce a (scale and time-dependent!) velocity bias. Our measurements of WL and RSD still map out the same metric potentials for our tracers, but these are not the complete potentials that the dark matter feels. Allowing for such deviations, we completely lose the connection between the dark matter growth rate and RSD of the galaxy power spectrum.

Summarizing the above, we can say that RSD and WL map out the Jordan-frame metric for galaxies and light, but provide no direct information on the Jordan frame of the underlying dark matter. In principle, one could use different tracers with different baryon fractions (cluster and galaxy power spectra) to map out the Jordan frames for these two classes of objects and obtain some information on the differences in the gravitational potentials they

experience (in the spirit of e.g. [44]). Interestingly, galaxies are not just baryons, but are dynamically coupled to their dark-matter halos. This means that the Jordan-frame metric for the galaxies is not necessarily the same as the one for baryons, since the galaxies will at least partly feel the fifth force acting on dark-matter.

Another interesting implication of our approach is that potential non-linearities of dark energy, which can appear on very different scales to those in dark matter as a result of the generic existence of screening mechanisms, are not deadly to the measurements of the linear potentials Φ and Ψ. For tracers to move on geodesics determined by these potentials, their gradients must remain small, i.e. the *total* EMT perturbations must be linear. So even if the DE contribution is non-linear, it is enough for the dark-matter density to be dominant and its perturbation linear for the tracers to continue to move on geodesics described by Φ and Ψ. However, since there will no doubt be non-linear contributions to the potentials, both from the DM and the DE perturbations, this should imply that measurements of higher-order correlation functions should be sensitive to the extra non-linearity as compared to the expected ΛCDM result.

There exist many, increasingly better, measurements of the bias b and the normalization σ_8 e.g. [98, 99, 100, 11, 101]. However, they all depend in a fundamental way on assumptions necessarily true only in ΛCDM and therefore we cannot use them. Although non-linearities can be used to constrain the bias through the galaxy bispectrum [101], this is a model-dependent statement since screening mechanisms present in most dark energy models alter the expectations. On the other hand, a measurement of bias is usually obtained as a result of measuring σ_8, which is done using either cluster counts and/or weak lensing around clusters. As we have already pointed out, weak lensing measures the lensing potential rather than the DM distribution, i.e. includes a dependence on dark energy perturbations. To extract information from cluster counts, their mass is obtained from their gas temperature—which gives information on the Newtonian potential Ψ and not on the DM mass—and spherical collapse or N-body simulations are used, both of which depend deeply on the model for dark energy, see e.g. Refs [102, 59, 103]. All of these issues can in principle be appropriately modeled, but this must be done on a model-by-model basis. For these reasons, we cannot interpret the ΛCDM measurement of σ_8 as a parameter valid for other models of dark energy.

The tests that we have constructed in chapter 6 depend on eliminating variables through the use of the constraints present in the Einstein equations. Given a class of models for DE, one can replace dynamical variables with combinations of observables. Given the assumption that the DE is a single degree of freedom, that the Equivalence Principle be satisfied and a detection of non-vanishing anisotropic stress, we have enough information to eliminate all non-observable quantities from the evolution equations and thus are able to form a null test

for the most general class of scalar-tensor models directly on the observable data.

When there is no anisotropic stress then no such complete constraint can be formed: the dependence on the unobservable $\delta_{\rm m}$ remains. In that case, the best that can be done is to obtain a measurement of the effective Newton's constant Y on the assumption that a particular class of models of dark energy describes the Universe and then use a consistency relation for Y to determine whether the assumption was consistent with the data. This is a somewhat more complicated exercise, which we have demonstrated for perfect-fluid k-*essence* models, but would also apply to imperfect-fluid models featuring kinetic gravity braiding [49, 59, 60].

Tests of the type we have shown can in principle be constructed for any other class of DE models. Indeed, we would like to argue that one should think of the parametrized or effective approaches, such as those of Refs [104, 105, 106, 107], as providing the dynamics of the dark energy which can be rewritten in terms of evolution equations for the potentials. Provided they are written in terms of parameters that on cosmological solutions are only functions of time, a test such as those presented in chapter 6 would allow for putting constraints on these parameters, or indeed would exclude setups which posses insufficient operators to describe the data fully.

An alternative way of thinking about these tests is that, using the measurement of Φ and Ψ, we are essentially reconstructing the components of an effective combined EMT for DM and DE [108]. Now, given a class of models, we can extract relations between the configuration of the degrees of freedom and the fluid variables, and therefore between the fluid variables themselves, i.e. anisotropic stress, pressure, energy density. In general this is difficult, but in some classes of models it can be done, e.g. [109, 32]. However, it should be intuitively clear that if the dark energy has more degrees of freedom, only the adiabatic modes will influence the potentials. Internal (isocurvature) modes, since they do not affect the gravitational field of the DE, would only be constrainable through their impact on the time evolution of the dark energy.

As we have discussed in the dark energy case, the impossibility to measure a gravitational coupling directly might force us to make a model-dependent analysis of this quantity, specially if anisotropic stress is not detected, indicating that we can not use an extra constrain from the general scalar-tensor model. However, this model-dependent analysis differs completely from the standard one that we have carried out in chapter 7 for a dark matter conversion model, because it consists on applying null-tests on data measured in multiple scales and reshifts.

By following the standard approach (Boltzmann code data fit), we have split the dark sector and have tested with large scale structure data the hypothesis of an environmental

conversion of cold dark matter into dark radiation that took place at late times in small scales. The results obtained within this (standard) model-dependent analysis point that the pure cold dark matter is a better option, although only marginally. Such analysis, as we have emphasized, exhibit degeneracies between parameters that come from the the fact that we are not dealing with observable quantities, and by making a split of the energy momentum tensor, one imposes strong priors on the type of dark energy. Moreover, this type of fit does not cover the full theoretical space, because the fiducial ΛCDM model does not exhibit, for instance, dark energy perturbations.

We would like to stress that the method we propose depends on taking derivatives of the data. Since for the purposes of this thesis we are working in the idealized case of sufficiently good data, we have not addressed here the feasibility of this procedure in a realistic situation. We leave this for future work.

We have also used a number of simplifying assumptions for the relation of measurements to the potentials. For example, the Kaiser formula (4.2.4), assumes not only linearity, but also a flat sky and ignores near-horizon effects. As shown by e.g. [37], the correction involve contributions from, for example, weak lensing, which would pollute the determination of the peculiar velocities of galaxies from RSDs. Indeed there are also near horizon corrections to the weak lensing, e.g. [110]. Since our aim is to exploit large-scale data fully, taking into account such corrections is a natural extension of this work.

Bibliography

[1] **Planck Collaboration** Collaboration, P. Ade *et al.*, "Planck 2013 results. XVI. Cosmological parameters," arXiv:1303.5076 [astro-ph.CO].

[2] A. Lewis, A. Challinor, and A. Lasenby, "Efficient computation of cosmic microwave background anisotropies in closed Friedmann-Robertson-Walker models," *The Astrophysical Journal* **538** no. 2, (2000) 473.

[3] J. Lesgourgues, "The Cosmic Linear Anisotropy Solving System (CLASS) I: Overview," arXiv:1104.2932 [astro-ph.IM].

[4] L. Amendola and S. Tsujikawa, *Dark Energy: Theory and Observations*. Cambridge University Press, 2010.

[5] P. J. E. Peebles and B. Ratra, "The cosmological constant and dark energy," *Rev. Mod. Phys.* **75** (Apr, 2003) 559–606. http://link.aps.org/doi/10.1103/RevModPhys.75.559.

[6] G. Steigman, "Neutrinos And Big Bang Nucleosynthesis," *Adv.High Energy Phys.* **2012** (2012) 268321, arXiv:1208.0032 [hep-ph].

[7] S. S. McGaugh, W. de Blok, J. Schombert, R. K. de Naray, and J. Kim, "The Rotation Velocity Attributable to Dark Matter at Intermediate Radii in Disk Galaxies," *Astrophys.J.* **659** (2007) 149–161, arXiv:astro-ph/0612410 [astro-ph].

[8] T. Clifton, P. G. Ferreira, A. Padilla, and C. Skordis, "Modified Gravity and Cosmology," *Phys.Rept.* **513** (2012) 1–189, arXiv:1106.2476 [astro-ph.CO].

[9] P. Peebles, "The mean mass density of the Universe,".

[10] E. Falco, C. Kochanek, and J. Munoz, "Limits on cosmological models from radio selected gravitational lenses," *Astrophys.J.* **494** (1998) 47–59, arXiv:astro-ph/9707032 [astro-ph].

[11] R. Mandelbaum, A. Slosar, T. Baldauf, U. Seljak, C. M. Hirata, *et al.*, "Cosmological parameter constraints from galaxy-galaxy lensing and galaxy clustering with the SDSS DR7," arXiv:1207.1120 [astro-ph.CO].

[12] S. Dodelson, *Modern Cosmology*. Academic Press, 2003.

[13] R. Durrer, "What do we really know about Dark Energy?," *Phil.Trans.Roy.Soc.Lond.* **A369** (2011) 5102–5114, arXiv:1103.5331 [astro-ph.CO].

[14] S. M. Carroll, "Dark energy and the preposterous universe," arXiv:astro-ph/0107571 [astro-ph].

[15] Z. Ahmed, D. Akerib, E. Armengaud, S. Arrenberg, C. Augier, C. Bailey, D. Balakishiyeva, L. Baudis, D. Bauer, A. Benoît, *et al.*, "Combined limits on WIMPs from the CDMS and EDELWEISS experiments," *Physical Review D* **84** no. 1, (2011) 011102.

[16] L. Bergstrom, "Dark Matter Evidence, Particle Physics Candidates and Detection Methods," *Annalen Phys.* **524** (2012) 479–496, arXiv:1205.4882 [astro-ph.HE].

[17] G. Bertone, D. Hooper, and J. Silk, "Particle dark matter: Evidence, candidates and constraints," *Phys.Rept.* **405** (2005) 279–390, arXiv:hep-ph/0404175 [hep-ph].

[18] A. S. Chou, W. Wester, A. Baumbaugh, H. R. Gustafson, Y. Irizarry-Valle, P. O. Mazur, J. H. Steffen, R. Tomlin, A. Upadhye, A. Weltman, X. Yang, and J. Yoo, "Search for Chameleon Particles Using a Photon-Regeneration Technique," *Phys. Rev. Lett.* **102** (Jan, 2009) 030402. http://link.aps.org/doi/10.1103/PhysRevLett.102.030402.

[19] G. Dvali and M. Zaldarriaga, "Changing alpha with time: Implications for fifth force type experiments and quintessence," *Phys.Rev.Lett.* **88** (2002) 091303, arXiv:hep-ph/0108217 [hep-ph].

[20] J. O'Bryan, J. Smidt, F. De Bernardis, and A. Cooray, "Constraints on Spatial Variations in the Fine-Structure constant from Planck," arXiv:1306.1232 [astro-ph.CO].

[21] C. M. Will, "The Confrontation between general relativity and experiment," *Living Rev.Rel.* **9** (2006) 3, arXiv:gr-qc/0510072 [gr-qc].

[22] J. Khoury and A. Weltman, "Chameleon cosmology," *Phys. Rev. D* **69** (Feb, 2004) 044026. http://link.aps.org/doi/10.1103/PhysRevD.69.044026.

[23] **GammeV Collaboration** Collaboration, J. H. Steffen *et al.*, "Laboratory constraints on chameleon dark energy and power-law fields," *Phys.Rev.Lett.* **105** (2010) 261803, arXiv:1010.0988 [astro-ph.CO].

[24] D. J. Schlegel, M. Blanton, D. Eisenstein, B. Gillespie, J. Gunn, P. Harding, P. McDonald, R. Nichol, N. Padmanabhan, W. Percival, *et al.*, "SDSS-III: The Baryon Oscillation Spectroscopic Survey (BOSS)," in *Bulletin of the American Astronomical Society*, vol. 38, p. 966. 2007.

[25] B. Flaugher, "The dark energy survey," *International Journal of Modern Physics A* **20** no. 14, (2005) 3121–3123.

[26] N. Kaisera, H. Aussela, B. Burkeb, H. Boesgaarda, K. Chambersa, M. Chunc, J. Heasleya, K. Hodappc, B. Huntd, R. J. D. Jewitta, *et al.*, "Pan-starrs—a large synoptic survey telescope array," in *Proc. of SPIE Vol*, vol. 4836, p. 155. 2002.

[27] R. J. Laureijs, L. Duvet, I. E. Sanz, P. Gondoin, D. H. Lumb, T. Oosterbroek, and G. S. Criado, "The Euclid Mission," in *SPIE Astronomical Telescopes and Instrumentation: Observational Frontiers of Astronomy for the New Decade*, pp. 77311H–77311H, International Society for Optics and Photonics. 2010.

[28] **Euclid Theory Working Group** Collaboration, L. Amendola *et al.*, "Cosmology and fundamental physics with the Euclid satellite," arXiv:1206.1225 [astro-ph.CO].

[29] L. Amendola, M. Kunz, M. Motta, I. D. Saltas, and I. Sawicki, "Observables and unobservables in dark energy cosmologies," *Phys.Rev.* **D87** (2013) 023501, arXiv:1210.0439 [astro-ph.CO].

[30] D. Boriero, P. de Holanda, and M. Motta, "Limits in late time conversion of cold dark matter into dark radiation," *Journal of Cosmology and Astroparticle Physics* **2013** no. 06, (2013) 006.

[31] M. Motta, I. Sawicki, I. D. Saltas, L. Amendola, and M. Kunz, "Probing Dark Energy through Scale Dependence," arXiv:1305.0008 [astro-ph.CO].

[32] I. Sawicki, I. D. Saltas, L. Amendola, and M. Kunz, "Consistent perturbations in an imperfect fluid," *JCAP* **1301** (2013) 004, arXiv:1208.4855 [astro-ph.CO].

[33] M. Kunz and D. Sapone, "Dark Energy versus Modified Gravity," *Phys. Rev. Lett.* **98** (Mar, 2007) 121301. http://link.aps.org/doi/10.1103/PhysRevLett.98.121301.

[34] W. Hu and N. Sugiyama, "Small scale cosmological perturbations: An Analytic approach," *Astrophys.J.* **471** (1996) 542–570, arXiv:astro-ph/9510117 [astro-ph].

[35] D. J. Eisenstein and W. Hu, "Baryonic features in the matter transfer function," *Astrophys.J.* **496** (1998) 605, arXiv:astro-ph/9709112 [astro-ph].

[36] M. Kunz, "The dark degeneracy: On the number and nature of dark components," *Phys.Rev.* **D80** (2009) 123001, arXiv:astro-ph/0702615 [astro-ph].

[37] C. Bonvin and R. Durrer, "What galaxy surveys really measure," *Phys.Rev.* **D84** (2011) 063505, arXiv:1105.5280 [astro-ph.CO].

[38] N. Kaiser, "Clustering in real space and in redshift space," *Mon.Not.Roy.Astron.Soc.* **227** (1987) 1–27.

[39] R. Scoccimarro, H. Couchman, and J. A. Frieman, "The Bispectrum as a signature of gravitational instability in redshift-space," *Astrophys.J.* **517** (1999) 531–540, arXiv:astro-ph/9808305 [astro-ph].

[40] V. Desjacques and R. K. Sheth, "Redshift space correlations and scale-dependent stochastic biasing of density peaks," *Phys.Rev.* **D81** (2010) 023526, arXiv:0909.4544 [astro-ph.CO].

[41] L. Amendola, "Coupled quintessence," *Phys.Rev.* **D62** (2000) 043511, arXiv:astro-ph/9908023 [astro-ph].

[42] E. Macaulay, H. A. Feldman, P. G. Ferreira, A. H. Jaffe, S. Agarwal, *et al.*, "Power Spectrum Estimation from Peculiar Velocity Catalogues," *Mon.Not.Roy.Astron.Soc.* **425** (2012) 1709–1717, arXiv:1111.3338 [astro-ph.CO].

[43] P. Zhang, M. Liguori, R. Bean, and S. Dodelson, "Probing Gravity at Cosmological Scales by Measurements which Test the Relationship between Gravitational Lensing and Matter Overdensity," *Phys.Rev.Lett.* **99** (2007) 141302, arXiv:0704.1932 [astro-ph].

[44] L. Hui and A. Nicolis, "Proposal for an Observational Test of the Vainshtein Mechanism," *Phys.Rev.Lett.* **109** (2012) 051304, arXiv:1201.1508 [astro-ph.CO].

[45] G.-B. Zhao, T. Giannantonio, L. Pogosian, A. Silvestri, D. J. Bacon, *et al.*, "Probing modifications of General Relativity using current cosmological observations," *Phys.Rev.* **D81** (2010) 103510, arXiv:1003.0001 [astro-ph.CO].

[46] A. Silvestri, L. Pogosian, and R. V. Buniy, "A practical approach to cosmological perturbations in modified gravity," arXiv:1302.1193 [astro-ph.CO].

[47] W. J. Percival and M. White, "Testing cosmological structure formation using redshift-space distortions," *Mon.Not.Roy.Astron.Soc.* **393** (2009) 297–308, arXiv:0808.0003 [astro-ph].

[48] G. W. Horndeski, "Second-order scalar-tensor field equations in a four-dimensional space," *Int.J.Th.Phys.* **10** (1974) 363–384.

[49] C. Deffayet, X. Gao, D. Steer, and G. Zahariade, "From k-essence to generalised Galileons," *Phys.Rev.* **D84** (2011) 064039, arXiv:1103.3260 [hep-th].

[50] C. Armendariz-Picon, T. Damour, and V. F. Mukhanov, "k - inflation," *Phys.Lett.* **B458** (1999) 209–218, arXiv:hep-th/9904075 [hep-th].

[51] C. Armendariz-Picon, V. F. Mukhanov, and P. J. Steinhardt, "A Dynamical solution to the problem of a small cosmological constant and late time cosmic acceleration," *Phys.Rev.Lett.* **85** (2000) 4438–4441, arXiv:astro-ph/0004134 [astro-ph].

[52] C. Armendariz-Picon, V. F. Mukhanov, and P. J. Steinhardt, "Essentials of k essence," *Phys.Rev.* **D63** (2001) 103510, arXiv:astro-ph/0006373 [astro-ph].

[53] J. Garriga and V. F. Mukhanov, "Perturbations in k-inflation," *Phys.Lett.* **B458** (1999) 219–225, arXiv:hep-th/9904176 [hep-th].

[54] V. Mukhanov, *Physical Foundations of Cosmology*. Cambridge Univ. Press, Cambridge.

[55] M. Kunz and D. Sapone, "Crossing the Phantom Divide," *Phys.Rev.* **D74** (2006) 123503, arXiv:astro-ph/0609040 [astro-ph].

[56] P. Creminelli, G. D'Amico, J. Norena, L. Senatore, and F. Vernizzi, "Spherical collapse in quintessence models with zero speed of sound," *JCAP* **1003** (2010) 027, arXiv:0911.2701 [astro-ph.CO].

[57] E. A. Lim, I. Sawicki, and A. Vikman, "Dust of Dark Energy," *JCAP* **1005** (2010) 012, arXiv:1003.5751 [astro-ph.CO].

[58] C. Deffayet, O. Pujolas, I. Sawicki, and A. Vikman, "Imperfect Dark Energy from Kinetic Gravity Braiding," *JCAP* **1010** (2010) 026, arXiv:1008.0048 [hep-th].

[59] R. Kimura and K. Yamamoto, "Large Scale Structures in Kinetic Gravity Braiding Model That Can Be Unbraided," *JCAP* **1104** (2011) 025, arXiv:1011.2006 [astro-ph.CO].

[60] O. Pujolas, I. Sawicki, and A. Vikman, "The Imperfect Fluid behind Kinetic Gravity Braiding," *JHEP* **1111** (2011) 156, arXiv:1103.5360 [hep-th].

[61] A. De Felice, T. Kobayashi, and S. Tsujikawa, "Effective gravitational couplings for cosmological perturbations in the most general scalar-tensor theories with second-order field equations," *Phys.Lett.* **B706** (2011) 123–133, arXiv:1108.4242 [gr-qc].

[62] I. D. Saltas and M. Kunz, "Anisotropic stress and stability in modified gravity models," *Phys.Rev.* **D83** (2011) 064042, arXiv:1012.3171 [gr-qc].

[63] A. De Felice and S. Tsujikawa, "f(R) theories," *Living Rev.Rel.* **13** (2010) 3, 1002.4928.

[64] W. Hu and I. Sawicki, "Models of f(R) Cosmic Acceleration that Evade Solar-System Tests," *Phys.Rev.* **D76** (2007) 064004, arXiv:0705.1158 [astro-ph].

[65] V. Springel, J. Wang, M. Vogelsberger, A. Ludlow, A. Jenkins, *et al.*, "The Aquarius Project: the subhalos of galactic halos," *Mon.Not.Roy.Astron.Soc.* **391** (2008) 1685–1711, arXiv:0809.0898 [astro-ph].

[66] A. V. Maccio', A. A. Dutton, F. C. van den Bosch, B. Moore, D. Potter, *et al.*, "Concentration, Spin and Shape of Dark Matter Haloes: Scatter and the Dependence on Mass and Environment," *Mon.Not.Roy.Astron.Soc.* **378** (2007) 55–71, arXiv:astro-ph/0608157 [astro-ph].

[67] S. Kazantzidis, E. L. Lokas, L. Mayer, A. Knebe, and J. Klimentowski, "Formation of Dwarf Spheroidal Galaxies Via Mergers of Disky Dwarfs," *Astrophys.J.* **740** (2011) L24–L29, arXiv:1108.3606 [astro-ph.CO].

[68] J. Wang, C. S. Frenk, and A. P. Cooper, "The Spatial Distribution of Galactic Satellites in the LCDM Cosmology," arXiv:1206.1340 [astro-ph.GA].

[69] M. Loewenstein and A. Kusenko, "Dark Matter Search Using Chandra Observations of Willman 1, and a Spectral Feature Consistent with a Decay Line of a 5 keV Sterile Neutrino," *Astrophys.J.* **714** (2010) 652–662, arXiv:0912.0552 [astro-ph.HE].

[70] A. V. Maccio, S. Paduroiu, D. Anderhalden, A. Schneider, and B. Moore, "Cores in warm dark matter haloes: a Catch 22 problem," arXiv:1202.1282 [astro-ph.CO].

[71] M. R. Lovell, V. Eke, C. S. Frenk, L. Gao, A. Jenkins, *et al.*, "The Haloes of Bright Satellite Galaxies in a Warm Dark Matter Universe," *Mon.Not.Roy.Astron.Soc.* **420** (2012) 2318–2324, arXiv:1104.2929 [astro-ph.CO].

[72] A. Doroshkevich, M. Khlopov, and A. Klypin, "Large-scale structure of the universe in unstable dark matter models," *Mon.Not.Roy.Astron.Soc.* **239** (1989) 923–938.

[73] L. E. Strigari, M. Kaplinghat, and J. S. Bullock, "Dark Matter Halos with Cores from Hierarchical Structure Formation," *Phys.Rev.* **D75** (2007) 061303, arXiv:astro-ph/0606281 [astro-ph].

[74] S. Trujillo-Gomez, A. Klypin, J. Primack, and A. J. Romanowsky, "Galaxies in LCDM with Halo Abundance Matching: luminosity-velocity relation, baryonic mass-velocity relation, velocity function and clustering," *Astrophys.J.* **742** (2011) 16, arXiv:1005.1289 [astro-ph.CO].

[75] S. Mashchenko, J. Wadsley, and H. M. P. Couchman, "Stellar Feedback in Dwarf Galaxy Formation," *Science* **319** no. 5860, (2008) 174–177, arXiv:0711.4803 [astro-ph]. http://www.sciencemag.org/content/319/5860/174.abstract.

[76] F. Governato, C. Brook, L. Mayer, A. Brooks, G. Rhee, *et al.*, "At the heart of the matter: the origin of bulgeless dwarf galaxies and Dark Matter cores," *Nature* **463** (2010) 203–206, arXiv:0911.2237 [astro-ph.CO].

[77] F. Governato, A. Zolotov, A. Pontzen, C. Christensen, S. Oh, *et al.*, "Cuspy No More: How Outflows Affect the Central Dark Matter and Baryon Distribution in Lambda CDM Galaxies," *Mon.Not.Roy.Astron.Soc.* **422** (2012) 1231–1240, arXiv:1202.0554 [astro-ph.CO].

[78] L. G. d. Aarssen, T. Bringmann, and C. Pfrommer, "Is dark matter with long-range interactions a solution to all small-scale problems of ΛCDM cosmology?," *Phys.Rev.Lett.* **109** (2012) 231301, arXiv:1205.5809 [astro-ph.CO].

[79] S. Hannestad, A. Mirizzi, G. G. Raffelt, and Y. Y. Wong, "Neutrino and axion hot dark matter bounds after WMAP-7," *JCAP* **1008** (2010) 001, arXiv:1004.0695 [astro-ph.CO].

[80] W. Fischler and J. Meyers, "Dark Radiation Emerging After Big Bang Nucleosynthesis?," *Phys.Rev.* **D83** (2011) 063520, arXiv:1011.3501 [astro-ph.CO].

[81] K. Choi, K.-Y. Choi, and C. S. Shin, "Dark radiation and small-scale structure problems with decaying particles," *Phys.Rev.* **D86** (2012) 083529, arXiv:1208.2496 [hep-ph].

[82] L. Amendola, M. Baldi, and C. Wetterich, "Quintessence cosmologies with a growing matter component," *Phys.Rev.* **D78** (2008) 023015, arXiv:arXiv:0706.3064 [astro-ph].

[83] Y. Ayaita, M. Weber, and C. Wetterich, "Neutrino Lump Fluid in Growing Neutrino Quintessence," arXiv:arXiv:1211.6589 [astro-ph.CO].

[84] P. Madau, L. Pozzetti, and M. Dickinson, "The Star formation history of field galaxies," *Astrophys.J.* **498** (1998) 106, arXiv:astro-ph/9708220 [astro-ph].

[85] C. Porciani and P. Madau, "On the Association of gamma-ray bursts with massive stars: implications for number counts and lensing statistics," *Astrophys.J.* **548** (2001) 522–531, arXiv:astro-ph/0008294 [astro-ph].

[86] S. Ando and K. Sato, "Relic neutrino background from cosmological supernovae," *New J.Phys.* **6** (2004) 170, arXiv:astro-ph/0410061 [astro-ph].

[87] S. Ando, J. F. Beacom, and H. Yuksel, "Detection of neutrinos from supernovae in nearby galaxies," *Phys.Rev.Lett.* **95** (2005) 171101, arXiv:astro-ph/0503321 [astro-ph].

[88] C. Lunardini, "The diffuse supernova neutrino flux, supernova rate and sn1987a," *Astropart.Phys.* **26** (2006) 190–201, arXiv:astro-ph/0509233 [astro-ph].

[89] E. E. Salpeter, "The Luminosity Function and Stellar Evolution.," *Apj* **121** (Jan., 1955) 161.

[90] A. Gould, J. N. Bahcall, and C. Flynn, "Disk M dwarf luminosity function from HST star counts," *Astrophys.J.* **465** (1996) 759, arXiv:astro-ph/9505087 [astro-ph].

[91] P. Madau, F. Haardt, and L. Pozzetti, "Extragalactic Background Light, MACHOs, and the Cosmic Stellar Baryon Budget," in *The Extragalactic Infrared Background and its Cosmological Implications*, M. Harwit and M. G. Hauser, eds., vol. 204 of *IAU Symposium*, p. 359. Jan., 2001. arXiv:astro-ph/0012271 [astro-ph].

[92] C.-P. Ma and E. Bertschinger, "Cosmological perturbation theory in the synchronous and conformal Newtonian gauges," *Astrophys. J.* **455** (1995) 7–25, astro-ph/9506072.

[93] A. Lewis and S. Bridle, "Cosmological parameters from CMB and other data: a Monte- Carlo approach," *Phys. Rev.* **D66** (2002) 103511, astro-ph/0205436. http://cosmologist.info/cosmomc.

[94] A. Lewis, A. Challinor, and A. Lasenby, "Efficient Computation of CMB anisotropies in closed FRW models," *Astrophys. J.* **538** (2000) 473–476, astro-ph/9911177. http://camb.info.

[95] S. Hannestad, "Neutrino masses and the dark energy equation of state - Relaxing the cosmological neutrino mass bound," *Phys.Rev.Lett.* **95** (2005) 221301, arXiv:astro-ph/0505551 [astro-ph].

[96] J. Hamann, S. Hannestad, G. Raffelt, and Y. Y. Wong, "Observational bounds on the cosmic radiation density," *JCAP* **0708** (2007) 021, arXiv:0705.0440 [astro-ph].

[97] W. de Blok, "The Core-Cusp Problem," *Adv.Astron.* **2010** (2010) 789293, arXiv:0910.3538 [astro-ph.CO].

[98] E. Rozo *et al.*, "Cosmological Constraints from the SDSS maxBCG Cluster Catalog," *Astrophys.J.* **708** (2010) 645–660, arXiv:0902.3702 [astro-ph.CO].

[99] J. L. Tinker, E. S. Sheldon, R. H. Wechsler, M. R. Becker, E. Rozo, *et al.*, "Cosmological Constraints from Galaxy Clustering and the Mass-to-Number Ratio of Galaxy Clusters," *Astrophys.J.* **745** (2012) 16, arXiv:1104.1635 [astro-ph.CO].

[100] R. Tojeiro, W. Percival, J. Brinkmann, J. Brownstein, D. Eisenstein, *et al.*, "The clustering of galaxies in the SDSS-III Baryon Oscillation Spectroscopic Survey: measuring structure growth using passive galaxies," *Mon.Not.Roy.Astron.Soc.* **424** (2012) 2339–2344, arXiv:1203.6565 [astro-ph.CO].

[101] **WiggleZ Collaboration** Collaboration, F. A. Marin *et al.*, "The WiggleZ Dark Energy Survey: constraining galaxy bias and cosmic growth with 3-point correlation functions," arXiv:1303.6644 [astro-ph.CO].

[102] F. Schmidt, W. Hu, and M. Lima, "Spherical Collapse and the Halo Model in Braneworld Gravity," *Phys.Rev.* **D81** (2010) 063005, arXiv:0911.5178 [astro-ph.CO].

[103] A. Borisov, B. Jain, and P. Zhang, "Spherical Collapse in f(R) Gravity," *Phys.Rev.* **D85** (2012) 063518, arXiv:1102.4839 [astro-ph.CO].

[104] T. Baker, P. G. Ferreira, and C. Skordis, "The Parameterized Post-Friedmann Framework for Theories of Modified Gravity: Concepts, Formalism and Examples," *Phys.Rev.* **D87** (2013) 024015, arXiv:1209.2117 [astro-ph.CO].

[105] G. Gubitosi, F. Piazza, and F. Vernizzi, "The Effective Field Theory of Dark Energy," *JCAP* **1302** (2013) 032, arXiv:1210.0201 [hep-th].

[106] J. K. Bloomfield, E. E. Flanagan, M. Park, and S. Watson, "Dark Energy or Modified Gravity? An Effective Field Theory Approach," arXiv:1211.7054 [astro-ph.CO].

[107] J. Gleyzes, D. Langlois, F. Piazza, and F. Vernizzi, "Essential Building Blocks of Dark Energy," arXiv:1304.4840 [hep-th].

[108] G. Ballesteros, L. Hollenstein, R. K. Jain, and M. Kunz, "Nonlinear cosmological consistency relations and effective matter stresses," *JCAP* **1205** (2012) 038, arXiv:1112.4837 [astro-ph.CO].

[109] R. A. Battye and J. A. Pearson, "Effective action approach to cosmological perturbations in dark energy and modified gravity," *JCAP* **1207** (2012) 019, arXiv:1203.0398 [hep-th].

[110] F. Bernardeau, C. Bonvin, and F. Vernizzi, "Full-sky lensing shear at second order," *Phys.Rev.* **D81** (2010) 083002, arXiv:0911.2244 [astro-ph.CO].

[111] A. De Felice and S. Tsujikawa, "Conditions for the cosmological viability of the most general scalar-tensor theories and their applications to extended Galileon dark energy models," *JCAP* **1202** (2012) 007, arXiv:1110.3878 [gr-qc].

Appendix A : Details of Horndeski

8.1 Equations of Motion

$$\delta T^0_0 \equiv A_1\dot{\Phi} + A_2\dot{\delta\phi} - \rho_m\dot{v} + A_3\frac{k^2}{a^2}\Phi + A_4\Psi + A_5\frac{k^2}{a^2}\chi + \left(A_6\frac{k^2}{a^2} - \mu\right)\delta\phi - \rho_m\delta = 0\,, \quad (8.1.1)$$

$$\begin{aligned}\delta T^i_i \equiv{}& B_1\ddot{\Phi} + B_2\ddot{\delta\phi} + B_3\dot{\Phi} + B_4\dot{\delta\phi} + B_5\dot{\Psi} + B_6\frac{k^2}{a^2}\Phi + \left(B_7\frac{k^2}{a^2} + 3\nu\right)\delta\phi \\ &+ \left(B_8\frac{k^2}{a^2} + B_9\right)\Psi + B_{10}\frac{k^2}{a^2}\dot{\chi} + B_{11}\frac{k^2}{a^2}\chi + 3\rho_m\dot{v} = 0\,,\end{aligned} \quad (8.1.2)$$

$$\delta T^0_i \equiv C_1\dot{\Phi} + C_2\dot{\delta\phi} + C_3\Psi + C_4\delta\phi + \rho_m v = 0\,, \quad (8.1.3)$$

$$\begin{aligned}\nabla^\mu T_{\mu\nu} \equiv{}& D_1\ddot{\Phi} + D_2\ddot{\delta\phi} + D_3\dot{\Phi} + D_4\dot{\delta\phi} + D_5\dot{\Psi} + D_6\frac{k^2}{a^2}\dot{\chi} \\ &+ \left(D_7\frac{k^2}{a^2} + D_8\right)\Phi + \left(D_9\frac{k^2}{a^2} - M^2\right)\delta\phi + \left(D_{10}\frac{k^2}{a^2} + D_{11}\right)\Psi + D_{12}\frac{k^2}{a^2}\chi = 0\,,\end{aligned} \quad (8.1.4)$$

$$\delta T^i_j - {}^1\!/_3\delta^i_j\delta T^k_k \equiv B_6\Phi + B_7\delta\phi + B_8\Psi + B_{10}\dot{\chi} + B_{11}\chi = 0 \quad (8.1.5)$$

8.1.1 Coefficients

$$\begin{aligned}&A_1 = 6\Theta, \qquad A_2 = -2(\Sigma + 3H\Theta)/\dot{\phi}, \qquad A_3 = 2\mathcal{G}_T, \\ &A_4 = 2\Sigma + \rho_m, \qquad A_5 = -2\Theta, A_6 = 2(\Theta - H\mathcal{G}_T)/\dot{\phi}, \qquad \mu = \mathcal{E}_{,\phi}\,,\end{aligned} \quad (8.1.6)$$

$$\begin{aligned}&B_1 = 6\mathcal{G}_T, \qquad B_2 = 6(\Theta - H\mathcal{G}_T)/\dot{\phi}, \qquad B_3 = 6(\dot{\mathcal{G}}_T + 3H\mathcal{G}_T), \\ &B_4 = 3\left[\left(4H\ddot{\phi} - 4\dot{H}\dot{\phi} - 6H^2\dot{\phi}\right)\mathcal{G}_T - 2H\dot{\phi}\,\dot{\mathcal{G}}_T - \left(4\ddot{\phi} - 6H\dot{\phi}\right)\Theta + 2\dot{\phi}\dot{\Theta} - \rho_m\dot{\phi}\right]/\dot{\phi}^2, \\ &B_5 = -6\Theta, B_6 = 2\mathcal{F}_T, \qquad B_7 = 2\left[\dot{\mathcal{G}}_T + H\left(\mathcal{G}_T - \mathcal{F}_T\right)\right]/\dot{\phi}, \qquad B_8 = 2\mathcal{G}_T, \\ &B_9 = -6(\dot{\Theta} + 3H\Theta), B_{10} = -2\mathcal{G}_T, \qquad B_{11} = -2(\dot{\mathcal{G}}_T + H\mathcal{G}_T), \qquad \nu = \mathcal{P}_{,\phi}\,,\end{aligned} \quad (8.1.7)$$

$$C_1 = 2\mathcal{G}_T, \qquad C_2 = 2(\Theta - H\mathcal{G}_T)/\dot{\phi}, \qquad C_3 = -2\Theta,$$
$$C_4 = \left[2(H\ddot{\phi} - \dot{H}\dot{\phi})\mathcal{G}_T - 2\ddot{\phi}\,\Theta - \rho_m\dot{\phi}\right]/\dot{\phi}^2, \tag{8.1.8}$$

$$D_1 = 6(\Theta - H\mathcal{G}_T)/\dot{\phi}, \qquad D_2 = 2(3H^2\mathcal{G}_T - 6H\Theta - \Sigma)/\dot{\phi}^2,$$
$$D_3 = -3\left[2H(\dot{\mathcal{G}}_T + 3H\mathcal{G}_T) - 2(\dot{\Theta} + 3H\Theta) - \rho_m\right]/\dot{\phi},$$
$$D_4 = 2[3H\{(3H^2 + 2\dot{H})\dot{\phi} - 2H\ddot{\phi}\}\mathcal{G}_T + 3H^2\dot{\phi}\dot{\mathcal{G}}_T + 6\{2H\ddot{\phi} - (3H^2 + \dot{H})\dot{\phi}\}\Theta - 6H\dot{\phi}\dot{\Theta}$$
$$+(2\ddot{\phi} - 3H\dot{\phi})\Sigma - \dot{\phi}\dot{\Sigma}]/\dot{\phi}^3,$$
$$D_5 = 2(\Sigma + 3H\Theta)/\dot{\phi}, \qquad D_6 = -2(\Theta - H\mathcal{G}_T)/\dot{\phi}, \qquad D_7 = 2\left[\dot{\mathcal{G}}_T + H\left(\mathcal{G}_T - \mathcal{F}_T\right)\right]/\dot{\phi}, \tag{8.1.9}$$
$$D_8 = 3\left[6(\dot{H}\dot{\phi} - H\ddot{\phi})\Theta - 2\ddot{\phi}\Sigma + 3H\rho_m\dot{\phi} - \mu\dot{\phi}^2\right]/\dot{\phi}^2,$$
$$D_9 = \left[2H^2\mathcal{F}_T - 4H(\dot{\mathcal{G}}_T + H\mathcal{G}_T) + 2(\dot{\Theta} + H\Theta) + \rho_m\right]/\dot{\phi}^2, \qquad D_{10} = 2(\Theta - H\mathcal{G}_T)/\dot{\phi},$$
$$D_{11} = [6\{(3H^2 + \dot{H})\dot{\phi} - H\ddot{\phi}\}\Theta + 6H\dot{\phi}\dot{\Theta} + 2(3H\dot{\phi} - \ddot{\phi})\Sigma + 2\dot{\phi}\dot{\Sigma} - \mu\dot{\phi}^2]/\dot{\phi}^2,$$
$$D_{12} = \left[2H(\dot{\mathcal{G}}_T + H\mathcal{G}_T) - 2(\dot{\Theta} + H\Theta) - \rho_m\right]/\dot{\phi}\,,$$

$$\begin{aligned}
M^2 &= \left[\dot{\mu} + 3H(\mu + \nu)\right]/\dot{\phi} \\
&= -K_{,\phi\phi} + (\ddot{\phi} + 3H\dot{\phi})K_{,\phi X} + 2XK_{,\phi\phi X} + 2X\ddot{\phi}K_{,\phi XX} \\
&+ [6\,H(G_{3,\phi XX}X + G_{3,\phi X})\dot{\phi} - 2\,G_{3,\phi\phi X}X - 2\,G_{3,\phi\phi}]\ddot{\phi} + 6\,H\,(G_{3,\phi\phi X}X - G_{3,\phi\phi})\,\dot{\phi} \\
&+ 6\,G_{3,\phi X}X\dot{H} + 2(9\,H^2G_{3,\phi X} - G_{3,\phi\phi\phi})X \\
&+ [6\,H^2(4\,G_{4,\phi XXX}X^2 + 8\,G_{4,\phi XX}X + G_{4,\phi X}) - 6\,H(2\,G_{4,\phi\phi XX}X + 3\,G_{4,\phi\phi X})\dot{\phi}]\ddot{\phi} \\
&+ [12\,H(G_{4,\phi X} + 2\,G_{4,\phi XX}X)\dot{H} + 6\,H(6\,H^2G_{4,\phi XX}X - 2\,G_{4,\phi\phi\phi X}X + 3\,H^2G_{4,\phi X})]\dot{\phi} \\
&+ 12\,H^2\left(2\,G_{4,\phi\phi XX}X^2 - 3\,G_{4,\phi\phi X}X - G_{4,\phi\phi}\right) - 6\,(2\,G_{4,\phi\phi X}X + G_{4,\phi\phi})\,\dot{H} \\
&+ [2H^3(2G_{5,\phi XXX}X^2 + 7G_{5,\phi XX}X + 3G_{5,\phi X})\dot{\phi} - 6H^2(5G_{5,\phi\phi X}X + G_{5,\phi\phi} + 2G_{5,\phi\phi XX}X^2)]\ddot{\phi} \\
&+ [2H^3(2\,G_{5,\phi\phi XX}X^2 - 9\,G_{5,\phi\phi} - 7\,G_{5,\phi\phi X}X) - 12\,H(G_{5,\phi\phi X}X + G_{5,\phi\phi})\dot{H}]\dot{\phi} \\
&+ 6H^2X\,(3G_{5,\phi X} + 2G_{5,\phi XX}X)\,\dot{H} + 6H^2X\left(3H^2G_{5,\phi X} - G_{5,\phi\phi\phi} + 2H^2G_{5,\phi XX}X - 2G_{5,\phi\phi\phi X}X\right).
\end{aligned}$$

where the functions $\mathcal{G}_T$,$\mathcal{F}_T$, $\Theta$and Σ are combinations of the Lagrangian functions that contain all its information, as presented in [111], with a different notation, w_i $(i = [1, 4])$. They are related as

$$
\begin{aligned}
\mathcal{G}_T \equiv w_1 \equiv & 2G_4 + 2XG_{5,\phi} - X\left(4G_{4,X} + 2HG_{5,X}\phi'\right) \\
2\Theta \equiv w_2 \equiv & 4G_4H + 2G_{4,\phi}\phi' + 2X\left(-8HG_{4,X} + 6HG_{5,\phi} - G_{3,X}\phi' + \right. \\
& \left. + 2G_{4,X\phi}\phi' - 5H^2G_{5,X}\phi'\right) + 4HX^2\left(-4G_{4,XX} + 2G_{5,X\phi} - HG_{5,XX}\phi'\right) \\
3\Sigma \equiv w_3 \equiv & -18G_4H^2 - 18HG_{4,\phi}\phi' + 3X(-2G_{3,\phi} + 18H^2G_{4,X} - \\
& 18H^2G_{5,\phi} + K_X) + \frac{3}{2}H^3G_{5,XXX}\left(\phi'\right)^7 + X^2\left(36\left(2H^2G_{4,XX} - H^2G_{5,\phi X}\right) + \right. \\
& + \frac{3}{2}H\left(12G_{3,XX} - 24G_{4,\phi XX} + 52H^2G_{5,XX}\right)\phi' + 36XH^2\left(2G_{4,XXX} - G_{5,\phi XX}\right)\Big) + \\
& + X\left(\frac{3}{2}\left(48H^2G_{4,X} - 36H^2G_{5,\phi}\right) + \frac{3}{2}\left(24HG_{3,X} - 60HG_{4\phi,X} + 60H^3G_{5,X}\right)\phi' + \right. \\
& \left. + \frac{3}{2}\left(-2G_{3,\phi X} + 72H^2G_{4,XX} - 42H^2G_{5,\phi X} + 2K_{XX}\right)\left(\phi'\right)^2\right) \\
\mathcal{F}_T \equiv w_4 \equiv & 2G_4 - 2X\left(G_{5,\phi} + G_{5,X}\phi''\right)
\end{aligned}
$$

We can also write the functions h_i from the quasi-static limit in terms of the w_i

$$
\begin{aligned}
h_1 &\equiv \frac{w_4}{w_1^2} = \frac{c_{\rm T}^2}{w_1} \qquad h_2 \equiv \frac{w_1}{w_4} = c_{\rm T}^{-2}\,, \\
h_3 &\equiv \frac{2w_1^2w_2H - w_2^2w_4 + 4w_1w_2w_1' - 2w_1^2(w_2' + \rho_m + 3H^2)}{2w_1^2M^2\dot{\varphi}^2} \\
h_4 &\equiv \frac{2w_1^2H^2 - w_2w_4H + 2w_1w_1'H + w_2w_1' - w_1(w_2' + \rho_m + 3H^2)}{2w_1^2M^2\dot{\varphi}^2} \\
h_5 &\equiv \frac{2w_1^2H^2 - w_2w_4H + 4w_1w_1'H + 2w_1'^2 - w_4(w_2' + \rho_m + 3H^2)}{M^2w_4\dot{\varphi}^2}
\end{aligned}
\tag{8.1.10}
$$

where the mass term is given in terms of derivatives of the total pressure and total energy with respect to the scalar.

$$
M^2 = \frac{3H\left(P_\phi + \varepsilon_\phi\right) + \dot{\varepsilon_\phi}}{\dot{\phi}}\,.
$$

Notice that the sound speed in [111] is given by

$$
c_{\rm s}^2 \equiv \frac{3(2w_1^2w_2H - w_2^2w_4 + 4w_1w_2w_1' - 2w_1^2(w_2' + \rho_{\rm m} + 3H^2))}{w_1(4w_1w_3 + 9w_2^2)}. \tag{8.1.11}
$$

and that we have an extra $3H^2$ compared to the reference due to the different definition of the Lagrangian.

8.2 The quasi-static limit of Horndeski

The modification of gravity in the Horndeski theory is accounted by a single extra scalar degree of freedom in addition to the Einstein Hilbert term, this means that we can obtain an evolution equation for the propagating scalar mode. By minimizing the linearly perturbed action for the scalar modes, an equation of motion for the perturbed scalar field and a series of constraints is obtained. Eliminating these constraints, we arrive at:

$$\left(k^4+\alpha_1 k^2\right)\Phi''+\left(\alpha_2 k^4+\alpha_3 k^2+\alpha_4\right)\Phi'+\left(\alpha_5 k^6+\alpha_6 k^4\alpha_7 k^2\right)\Phi= \tag{8.2.1}$$

$$\left(\alpha_8 k^2+\alpha_9\right)\delta'+\left(\alpha_{10}k^4+\alpha_{11}k^2\right)\delta \tag{8.2.2}$$

or, better expressed like:

$$\Phi''+\frac{\alpha_2 k^4+\alpha_3 k^2+\alpha_4}{k^4+\alpha_1 k^2}\Phi'+\frac{\alpha_5 k^4+\alpha_6 k^2+\alpha_7}{k^2+\alpha_1}\Phi= \tag{8.2.3}$$

$$\frac{\alpha_8 k^2+\alpha_9}{k^4+\alpha_1 k^2}\delta'+\frac{\alpha_{10}k^2+\alpha_{11}}{k^2+\alpha_1}\delta \tag{8.2.4}$$

The sound speed is defined in the limit $k\to\infty$, therefore $c_s^2\equiv\alpha_5$.

$$\Phi''+\alpha_2\left(1+\frac{\alpha_3}{\alpha_2 k^2}+\frac{\alpha_4}{\alpha_2 k^4}\right)\Phi'+c_s^2k^2\left(1+\frac{\alpha_6}{c_s^2k^2}+\frac{\alpha_7}{c_s^2k^4}\right)\Phi \tag{8.2.5}$$

$$\left(\frac{\alpha_8}{k^2}+\frac{\alpha_9}{k^4}\right)\delta'+\alpha_{10}\left(1+\frac{\alpha_{11}}{\alpha_{10}k^2}\right)\delta \tag{8.2.6}$$

In the subhorizon approximation, Eq.(8.2.5) reduces to

$$\Phi''+\alpha_2\left(1+\frac{\alpha_3-\xi_3}{\alpha_2 k^2}\right)\Phi'+c_s^2k^2\left(1+\frac{\alpha_6}{c_s^2k^2}+\frac{\alpha_7}{c_s^2k^4}\right)\Phi= \tag{8.2.7}$$

$$\alpha_{10}\left(1+\frac{\alpha_{11}}{\alpha_{10}k^2}\right)\delta \tag{8.2.8}$$

where ξ_3 is a term that comes explicitly from the equation of motion $E_\delta\equiv\delta_{\rm m}'+H^{-1}\theta_{\rm m}=-3\Phi'$. , used for the θ, which is dropped in the subhubble approximation.

In [61], it is argued that the mass of the scalar mode is related to the linear coefficient of $\delta\phi$, defined as M^2, in the equation of motion for the scalar perturbations. M^2corresponding to the mass of a canonical scalar field, described by the Lagrangian $L=X-V(\phi)$, with

$G_i = 0$, $i = 1, 2, 3$. It is also argued that in viable models based on $f(R)$ gravity and Brans-Dicke theory with a field potential, the term $-K$, is the dominant contribution to M^2, where this mass can become larger in early cosmological times and might induce oscillations in $\delta\phi$. It is expected that, if the oscillations are initially suppressed relative to the matter-induced mode, the quasi-static approximation can reproduce numerically integrated solutions with high accuracy. Based on these arguments, the authors derive the solutions keeping the M^2in the quasi-static e.o.m. for the perturbed field. We write explicitly these terms in the coefficients through the definition $\alpha_i \equiv \hat{\alpha}_i + M^2\beta_i$

$$\Phi'' + \alpha_2\left(1 + \frac{\hat{\alpha}_3 + M^2\beta_3 - \xi_3}{\alpha_2 k^2}\right)\Phi' + c_s^2 k^2\left(1 + \frac{\hat{\alpha}_6 + M^2\beta_6}{c_s^2 k^2} + \frac{\hat{\alpha}_7 + M^2\beta_7}{c_s^2 k^4}\right)\Phi = \tag{8.2.9}$$

$$\alpha_{10}k^2\left(1 + \frac{\hat{\alpha}_{11} + M^2\beta_{11}}{\alpha_{10}k^2}\right)\delta \tag{8.2.10}$$

Neglecting the time derivatives of the potential, we have

$$c_s^2 k^2\left(1 + \frac{\hat{\alpha}_6 + M^2\beta_6}{c_s^2 k^2} + \frac{\hat{\alpha}_7 + M^2\beta_7}{c_s^2 k^4}\right)\Phi = \alpha_{10}k^2\left(1 + \frac{\hat{\alpha}_{11} + M^2\beta_{11}}{\alpha_{10}k^2}\right)\delta \tag{8.2.11}$$

And keeping only the highest powers in k that are coefficients of M^2or δ leads to

$$c_s^2 k^2\left(1 + \frac{M^2\beta_6}{c_s^2 k^2}\right)\Phi = \alpha_{10}k^2\left(1 + \frac{M^2\beta_{11}}{\alpha_{10}k^2}\right)\delta \tag{8.2.12}$$

$$\Phi k^2 = \delta\frac{\alpha_{10}k^2 + \beta_{11}M^2}{c_s^2 k^2 + \beta_6 M^2} \tag{8.2.13}$$

$$\Phi = \frac{\alpha_{10}k^2 + \beta_{11}M^2}{c_s^2 k^4 + \beta_6 M^2 k^2}\delta \tag{8.2.14}$$

From the momentum, Hamiltonian and anisotropy constraints, we obtain

$$\left(k^4 + \gamma_1 k^2\right)\Psi + \left(\gamma_2 k^4 + \gamma_3 k^2\right)\Phi + \left(\gamma_4 k^2 + \gamma_5\right)\Phi' = \gamma_7 k^2\delta + \gamma_6\delta' \tag{8.2.15}$$

where no coefficient contains M^2 terms. In the subhuble scales, this approximates as

$$\left(k^2 + \gamma_1\right)\Psi + \left(\gamma_2 k^2 + \gamma_3\right)\Phi + \gamma_4\Phi' = \gamma_7\delta + \gamma_6\delta' \tag{8.2.16}$$

Neglecting time-derivatives of Φ and keeping the highest order terms in k takes to

$$k^2\left(\Psi+\gamma_2\Phi\right)=\gamma_7\delta \tag{8.2.17}$$

substituting the potential Φ from Eq.(8.2.13)

$$\Psi k^2+\gamma_2\delta\frac{\alpha_{10}k^2+\beta_{11}M^2}{c_s^2k^2+\beta_6M^2}=\gamma_7\delta \tag{8.2.18}$$

$$\Psi k^2=\left(\gamma_7-\gamma_2\frac{\alpha_{10}k^2+\beta_{11}M^2}{c_s^2k^2+\beta_6M^2}\right)\delta \tag{8.2.19}$$

$$\Psi k^2=\left(\frac{\left(\gamma_7c_s^2-\gamma_2\alpha_{10}\right)k^2+\left(\gamma_7\beta_6-\gamma_2\beta_{11}\right)M^2}{c_s^2k^2+\beta_6M^2}\right)\delta \tag{8.2.20}$$

The effective gravitational coupling

$$Y=-\frac{2}{3\Omega_m}\frac{\left(\gamma_7c_s^2-\gamma_2\alpha_{10}\right)k^2+\left(\gamma_7\beta_6-\gamma_2\beta_{11}\right)M^2}{c_s^2k^2+\beta_6M^2} \tag{8.2.21}$$

From Eq.(8.2.13) and Eq.(8.2.20), we obtain the the anisotropic stres

$$\eta\equiv-\frac{\Phi}{\Psi}=\frac{\alpha_{10}k^2+\beta_{11}M^2}{\left(\gamma_7c_s^2-\gamma_2\alpha_{10}\right)k^2+\left(\gamma_7\beta_6-\gamma_2\beta_{11}\right)M^2} \tag{8.2.22}$$

So we have recovered the result in [61] where the two quantities η and Y are described by a scale dependence of the form

$$Y=h_1\left(\frac{1+k^2h_5}{1+k^2h_3}\right), \tag{8.2.23}$$

$$\eta=h_2\left(\frac{1+k^2h_4}{1+k^2h_5}\right), \tag{8.2.24}$$